

## **SUPPORTING INFORMATION**

### ***Sequence-Controlled Copolymers of 2,3,4,5-Pentafluorostyrene: a Mechanistic Insight and Application to Organocatalysis***

John-Paul O'Shea,<sup>†</sup> Vera Solovyeva,<sup>†</sup> Xianrong Guo,<sup>‡</sup> Junpeng Zhao,<sup>†</sup> Nikos Hadjichristidis,<sup>†</sup> Valentin O. Rodionov.<sup>†\*</sup>

King Abdullah University of Science and Technology, Thuwal, 23955-6900, Kingdom of Saudi Arabia.

<sup>†</sup> KAUST Catalysis Center and Division of Physical Sciences and Engineering

<sup>‡</sup> KAUST Analytical Core Laboratories

## Contents

1. Nomenclature and abbreviations .....	3
2. Materials and methods .....	4
Materials: .....	4
Gas Chromatography - Mass Spectrometry:.....	4
Size Exclusion Chromatography: .....	4
Dynamic Light Scattering: .....	4
Differential Scanning Calorimetry (DSC): .....	4
Vapor-pressure Osmometry (VPO):.....	5
Nuclear Magnetic Resonance Spectroscopy (NMR): .....	5
ATR-FTIR:.....	5
UV-Vis:.....	5
3. Synthesis of small molecules .....	6
General notes. ....	6
4-azidomethyl styrene. ....	6
Sodium propargyl sulfonate.....	6
3-(trimethylsilyl)prop-2-yn-1-yl 2-bromo-2-methylpropanoate, TP.....	6
2-bromo-2-methyl-N-(prop-2-yn-1-yl)propanamide, BP .....	7
4. Determination of equilibrium constants for co-monomer complex formation, <b>K<sub>C</sub></b> .....	8
5. General ATRP methods and copolymerization kinetics.....	12
6. Determination of reactivity ratios .....	16
Reactivity ratios determined from ATRP:.....	16
Reactivity ratios determined from FRP: .....	17
Determination of monomer conversion: .....	17
Determination of polymer composition: .....	17
Determination of Fineman-Ross reactivity ratios:.....	17
Determination of reactivity ratios with complex contribution (Karad-Schneider): .....	19
7. Identification of liquid domains by DLS .....	23
8. Glass transition temperatures of various St-FSt copolymers.....	24
9. Determining the alternation mode of copolymers by HMBC NMR.....	25
10. Functionalization of P(N <sub>3</sub> St-alt-FSt) copolymer and catalysis .....	42
General procedure for cysteamine attachment by thiol substitution of para-F of FSt.....	42
General procedure for sulfonate attachment by CuAAC onto N <sub>3</sub> St moiety of the polymer.....	43
Check of primary-amine stability of the cysteamine residue by reaction with FITC.....	44
Observation of changes in physical appearance of the polymer during functionalization .....	45
General procedure for the Henry reactions.....	46
11. References.....	47

# 1. Nomenclature and abbreviations

Table 1. Nomenclature and abbreviations

Abbreviation	Name/description
AIBN	2,2'-azobis(2-methylpropionitrile)
ATRP	atom transfer radical polymerization
BP	2-bromo-2-methyl-N-(prop-2-yn-1-yl)propanamide
BPO	benzoyl peroxide
BPO-DMA	benzoyl peroxide/dimethylaniline
CB	chlorobenzene
CuAAC	copper-catalyzed azide-alkyne cycloaddition
DEE	diethyl ether
DLS	dynamic light scattering
DMF	N,N-dimethylformamide
DMSO	dimethylsulfoxide
FITC	fluorescein 5-isothiocyanate
FRP	free radical polymerization
FSt	1,2,3,4,5-pentafluorostyrene
GCMS	gas-chromatography mass-spectrometry
SEC	size exclusion chromatography
HMBC	heteronuclear multiple-bond correlation spectroscopy
$M_n$	number-average molecular weight
$M_w$	weight-average molecular weight
$N_3St$	4-azidomethyl styrene
PDI	polydispersity index
PMDETA	N, N, N', N', N'-pentamethyldiethylenetriamine
St	styrene
t-BP	tertiary butylperoxy pivalate
TEA	triethylamine
TEM	transmission electron microscopy
TFT	$\alpha,\alpha,\alpha$ -trifluorotoluene
THF	tetrahydrofuran
TLC	thin layer chromatography
TP	3-(trimethylsilyl)prop-2-yn-1-yl 2-bromo-2-methylpropanoate

## 2. Materials and methods

### *Materials:*

All reagents and solvents were provided by commercial suppliers (Sigma-Aldrich, Fisher Scientific and VWR) and used without further purification, unless otherwise noted. Monomer inhibitors were removed by passing the monomers through a column of neutral alumina and used immediately. Copper(I) bromide (CuBr) was purified by successive washings in glacial acetic acid, absolute ethanol and petroleum ether, and subsequently dried under vacuum for 24 hours.

### *Gas Chromatography - Mass Spectrometry:*

GC-MS analyses were performed on an Agilent 7820A gas chromatograph equipped with a 30m x 0.25mm HP-5MS capillary column (25 $\mu$  film thickness) and an Agilent 5975C mass-selective detector. Monomer conversion was determined by monitoring the decrease in the area of the corresponding monomer peak relative to hexadecane internal standard peak. The characteristic m/z values used for quantitation are as follows: N<sub>3</sub>St, 159.1; FSt, 194.1; St, 104.1; hexadecane, 85.1.

### *Size Exclusion Chromatography:*

Molecular weight and molecular weight distribution of polymers was determined from SEC using an Agilent liquid chromatography system fitted with refractive index (RID) and UV-Vis detectors, using two identical PLgel columns (5  $\mu$ m, MIXED-C) in connected series with THF as the mobile phase (1 mL/min). The column and flow path were temperature controlled at 25°C. Data analysis was performed using GPC-Addon for ChemStation software from Agilent. Narrow PDI poly(St) and poly(FSt) standards were prepared by ATRP using TPMP initiator. The degree of polymerization was determined by <sup>1</sup>H NMR from the ratio of the integral of the -CH<sub>2</sub>- backbone and trimethylsilyl end-group resonances. These standards were used for molecular weight calibration of the SEC system.

### *Dynamic Light Scattering:*

DLS measurements were performed to determine the size distribution of monomer aggregates in solution or bulk using a Malvern Zetasizer Nano ZS instrument equipped with a 632.8 nm He-Ne laser. The measurement angle was 173°. The cells were temperature controlled at 25  $\pm$  0.1 °C.

### *Differential Scanning Calorimetry (DSC):*

The glass transition and melting temperatures were measured using a Mettler Toledo DSC1 Star System differential scanning calorimeter. The samples (between 4 and 5 mg) in pre-weighed perforated aluminum capsules were heated at a rate of 10 °C/min (method: 40  $\rightarrow$  150  $\rightarrow$  -80  $\rightarrow$  150  $\rightarrow$  -80  $\rightarrow$  150  $\rightarrow$  -80  $\rightarrow$  150  $\rightarrow$  40 °C) under the flow of nitrogen. Transitions were recorded from the 2<sup>nd</sup> and 3<sup>rd</sup> heating cycles, and found from the midpoint of the onset and end-points. Two separate samples for each polymer were analyzed, and at least two repetitions were made for each sample.

#### *Vapor-pressure Osmometry (VPO):*

Number-average molecular weights ( $M_n$ ) were determined using a Gonotec Osmomat 070 VPO instrument in toluene at 41°C. Polymer concentrations for analysis ranged between 10 to 60 g polymer/kg solution. Instrument calibration was performed using benzil.

#### *Nuclear Magnetic Resonance Spectroscopy (NMR):*

Data for determining polymerization kinetics, as well as for routine characterization of small molecules, was recorded at room temperature on a Bruker Avance-III 400 MHz ( $^1\text{H}$ ) NMR spectrometer equipped with a Z-axis gradient BBO probe. NMR chemical shifts are reported in ppm and are calibrated against residual solvent signals of  $\text{CDCl}_3$  ( $\delta$  7.26, 77.16).

All 2D NMR spectra (HMBC and HMQC), as well as  $^1\text{H}$  and  $^{13}\text{C}$  spectra for all polymer samples, were obtained at room temperature on a Bruker AVANCE-III 950 MHz ( $^1\text{H}$ ) NMR instrument, equipped with a 5mm Z-axis gradient TCI cryoprobe.

Bruker standard **hmbcgp1ndqf** pulse program with QF acquisition mode in  $^{13}\text{C}$  dimension was applied when collecting the HMBC raw data. Bruker Topspin 3.0 was used as the processing software. To smooth the profile of the  $^{13}\text{C}$  projection, the following procedure was applied to all the HMBC spectra during processing. 256 data points (256 FIDs) were used for  $^{13}\text{C}$  dimension processing. Forward linear prediction to double the data points and then zero filling to 128k points were executed before the application of a Fourier transform. 1k data points were Fourier transformed in  $^1\text{H}$  dimension to restrict the size of the spectra. After Fourier transform, baseline correction and chemical shift calibration, the  $^{13}\text{C}$  projection was calculated ranging from 6.0 ppm to 7.5 ppm (for FSt/St copolymers), or from 6.0 ppm to 7.5 ppm (for FSt/ $\text{N}_3\text{St}$ ) in  $^1\text{H}$  dimension.

#### *ATR-FTIR:*

Data was collected on a Thermo Scientific Nicolet 6700 instrument equipped with nitrogen purge and aligned for signal clarity. The instrument was calibrated before sampling against a newly cleaned (acetone) and dried crystal surface. Solid polymer samples were placed directly on the crystal and secured with the needle press. Scans (32) from 4000 to 550  $\text{cm}^{-1}$  were recorded.

#### *UV-Vis:*

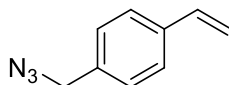
Data was collected in DMSO solutions on a Jasco V-670 instrument using air as the reference.

### 3. Synthesis of small molecules

#### General notes.

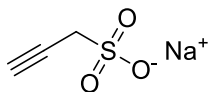
The following solutions have been used to stain TLC plates: ammonium molybdate/H<sub>2</sub>O, anisaldehyde/ethanol, and KMnO<sub>4</sub>/H<sub>2</sub>O. Preparative TLC was performed on 2000 μm silica gel plates (Analtech, Newark, DE). The bands were visualized with UV light, and products were extracted with 20% v/v methanol/dichloromethane. Flash chromatography was performed using Merck Kieselgel 60 (230-400 mesh) silica. Reactions requiring anhydrous conditions were performed under nitrogen or argon using standard Schlenk line techniques.

#### 4-azidomethyl styrene.



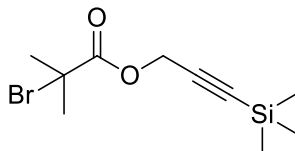
A similar method to that reported previously has been followed: <sup>1</sup> 4-chloromethyl styrene (23.8 g, 156 mmol, 1 equiv., *CMS*), NaN<sub>3</sub> (40.8 g, 624 mmol, 4 equiv.) were stirred in DMF (200 mL) at room temperature for 48 hours in a foil covered flask. Water (200 mL) was added. The product was extracted with DEE (3 x 100 mL). The organic phase was washed with brine containing 1 % m/m LiCl (3 x 100 mL) and then dried over magnesium sulfate, to yield a light yellow solution. Purification through a short column of basic alumina and subsequent concentration yielded clear, yellow tinged oil, (95% yield, 99.9% pure by GCMS, EI m/z: 159.1, 131.05, 130.1, 117.05, 104.05, 103, 102, 77, 51). ATR-FTIR (cm<sup>-1</sup>): 2091, 1511, 1407, 1343, 1249, 1205, 989, 909, 847, 822, 767, 718, 669. <sup>1</sup>H NMR (400 MHz, CDCl<sub>3</sub>, δ, ppm) 7.46 – 7.41 (m, 1H), 7.31 – 7.26 (m, 1H), 6.73 (dd, *J* = 17.6, 10.9 Hz, 1H), 5.78 (d, *J* = 17.6 Hz, 1H), 5.29 (d, *J* = 10.9 Hz, 1H), 4.33 (s, 1H). <sup>13</sup>C NMR (101 MHz, CDCl<sub>3</sub>, δ, ppm) δ 138.10, 136.66, 135.23, 128.91, 127.09, 114.92, 54.99.

#### Sodium propargyl sulfonate.



Following a method reported previously,<sup>1</sup> propargyl bromide (10 mL of 80 % toluene solution, 90 mmol, 1 eq.), sodium sulfite (14.26 g, 113 mmol, 1.26 eq.) were dissolved in a mixture of MeOH and water (1:1, 70 mL). The mixture was stirred at 65°C overnight. The mixture was cooled to room temperature and MeOH (500 mL) was added and the mixture was filtered to remove the precipitate. The filtrate was concentrated to produce a viscous liquid which precipitated a white material when acetone was added. <sup>1</sup>H NMR (400 MHz, D<sub>2</sub>O) δ 3.69 (d, 2H), 2.56 (t, 1H).

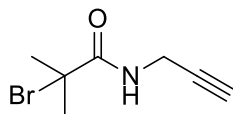
#### 3-(trimethylsilyl)prop-2-yn-1-yl 2-bromo-2-methylpropanoate, TP.



This compound was prepared in a 2-step procedure from propargyl alcohol according to reported procedures.<sup>2-5</sup> n-Butyl lithium (130.8 mL of 2.5 M in n-hexane, 327 mmol, 2.2 eq.) was added to a solution of propargyl alcohol (8.41 g, 8.73 mL, 150 mmol, 1 eq.) in THF (80 mL) at -78°C under nitrogen flow. The solution was stirred for 2 hours at this temperature. Subsequently trimethylsilyl chlo-

ride (TMS-Cl, 35.53 g, 41.5 mL, 327 mmol, 2.2 eq.) was added and the reaction was stirred for 30 min at room temperature. HCl (184.5 mL of 2 M, 369 mmol, 2.46 eq.) was slowly added and the resulting solution stirred for approximately 18 hours. The reaction mixture was cooled and neutralized carefully with the slow addition of saturated sodium bicarbonate ( $\text{NaHCO}_3$ ) and subsequently extracted with DEE (5 x 500 ml), dried over  $\text{MgSO}_4$ , concentrated under vacuum. GCMS and TLC revealed a pure product (TLC  $r_f = 18/45$ ) The 3-(trimethyl silyl) propargyl alcohol (5 g, 39 mmol, 1 eq.) was diluted with dry THF (150 mL), mixed with TEA (5.13 g, 7.06 mL, 51 mmol, 1.3 eq.) and cooled to  $0^\circ\text{C}$ . 2-Bromoisobutyryl bromide (11.72 g, 6.3 mL, 51 mmol, 1.3 eq.) diluted with THF (50 mL) was added drop-wise under nitrogen. The reaction was stirred for a further 18 hours and allowed to come to room temperature over the course of that period. The resultant reaction mixture was a dispersion of product with TEA-salt. The mixture was filtered through filter-agent to remove the salt. Water (200 mL) was added to the filtrate. The mixture was carefully titrated to  $\sim\text{pH } 9$  and extracted with DEE. The organic extract was washed with brine, dried over  $\text{MgSO}_4$  and purified by column chromatography (25:75 ethyl acetate: n-hexane, silica gel,  $r_f = 31/45$ ) to yield a viscous slightly yellow liquid.  $^1\text{H NMR}$  (400 MHz,  $\text{CDCl}_3$ ,  $\delta$ , ppm) 0.1 (s, 9), 1.9 (s, 6), 4.7 (s, 2).  $^{13}\text{C NMR}$  ( $\text{CDCl}_3$ ,  $\delta$ , ppm) 31.02, 54.60, 55.50, 93.14, 98.50, 171.23.

*2-bromo-2-methyl-N-(prop-2-yn-1-yl)propanamide, BP*



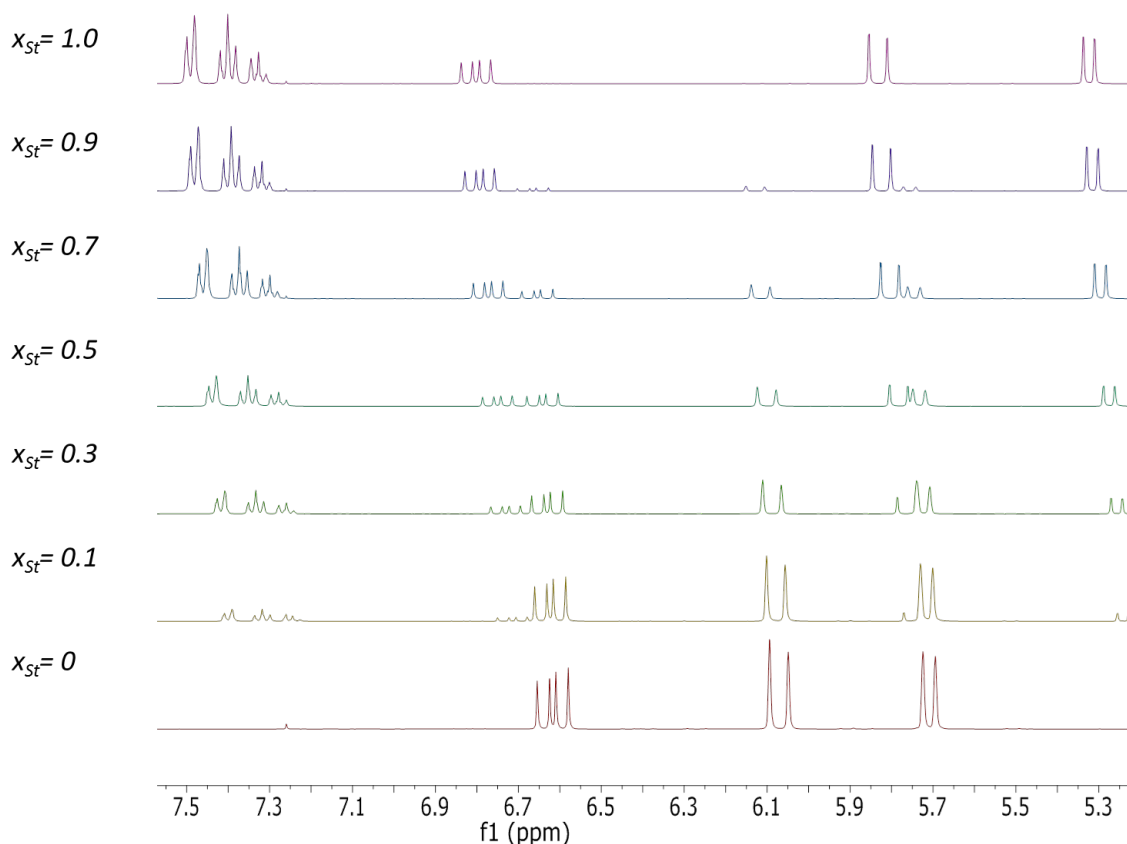
Diluted 2-bromoisobutyryl bromide (1.1 eq., dilution factor of 10 in dry THF) was added dropwise under nitrogen flow to a mixture of propargylamine (1 eq.) and TEA (1.2 eq.) in dry THF at  $0^\circ\text{C}$ . After addition was complete (60 min., dropwise), the mixture was allowed to stir at room temperature overnight. The resultant dispersion of reaction mixture and TEA-salt was filtered through a packed bed of filter agent. The clear filtrate was diluted with water (200 mL) and titrated to  $\sim\text{pH } 9$  and extracted with DEE (3 x 100 mL). The organic fraction was washed with brine (3 x 50 mL) and dried over  $\text{MgSO}_4$ . The mixture was concentrated under vacuum. A volume of DEE equivalent to the liquid residue was added and the product was crystallized at  $5^\circ\text{C}$ . The product was recrystallized from THF/DEE 1:5 a further 2 times to yield an off-white solid with a faint smell of rye bread.  $^1\text{H NMR}$  (400 MHz,  $\text{CDCl}_3$ ,  $\delta$ , ppm) 6.89 (broad, 1H, NH), 4.05 (m, 2H,  $-\text{NHCH}_2\text{CCH}$ ), 2.27 (t, 1H,  $-\text{NHCH}_2\text{CCH}$ ), 1.95 (s, 6H,  $-\text{C}(\text{CH}_3)_2\text{Br}$ ).  $^{13}\text{C NMR}$  ( $\text{CDCl}_3$ )  $\delta$  172.19, 79.31, 72.51, 62.59, 32.87, 30.69. ATR-FTIR ( $\text{cm}^{-1}$ ) 3299, 2123, 1660, 1523, 585.

## 4. Determination of equilibrium constants for co-monomer complex formation, $K_C$

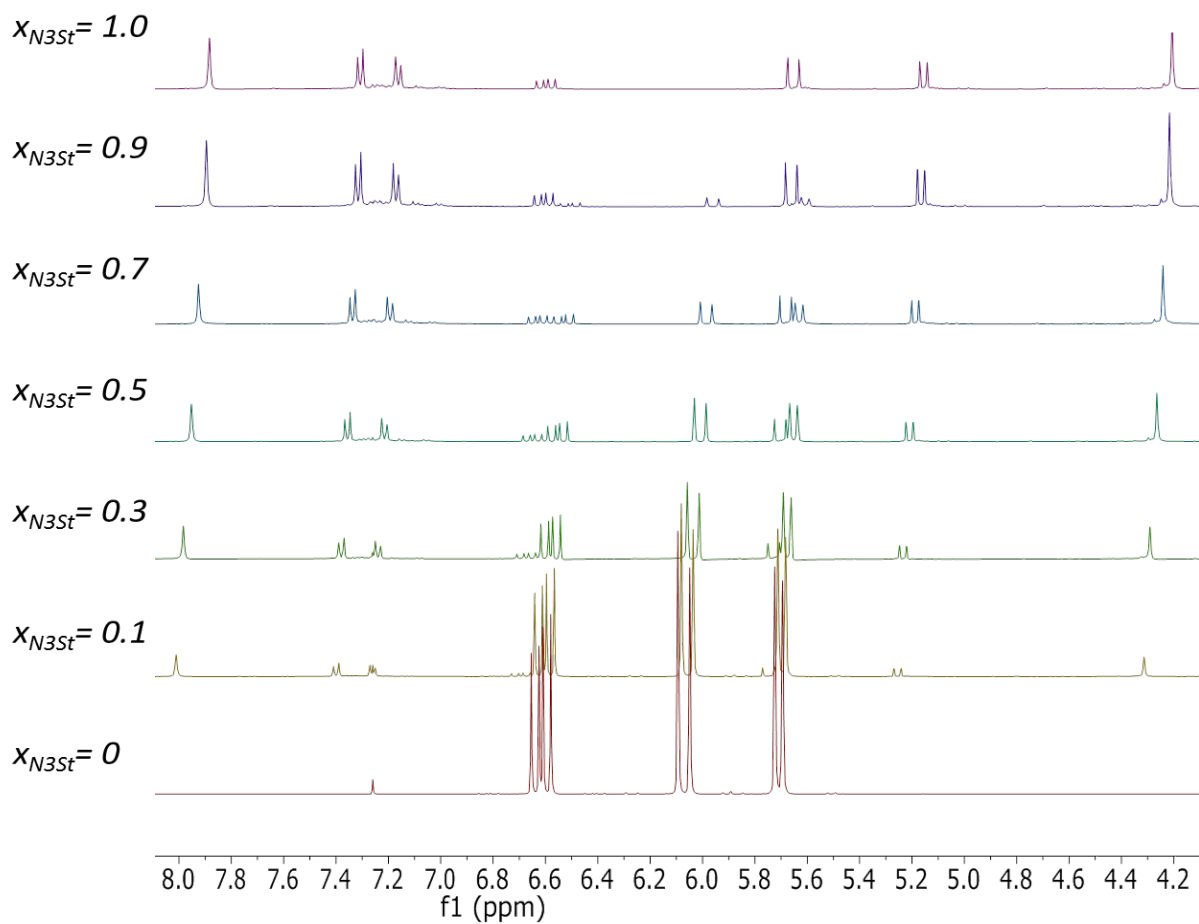
Numerous methods techniques could be used for observing the formation of co-monomer complexes: UV-Vis, DSC, visual observation, or NMR.<sup>6</sup> No wavelength shifts of absorbance of the co-monomer mixtures (as 0.001 M solutions in  $\text{CDCl}_3$ ) compared to the monomers was observed by UV-Vis (monomer absorbances :FSt-  $\lambda_{\text{max}} \sim 280$  nm; St -  $\lambda_{\text{max}} \sim 280$  nm;  $\text{N}_3\text{St}$  -  $\lambda_{\text{max}} \sim 280$  nm,  $\lambda_{\text{shoulder}} \sim 330$  nm, none of these values change when molar ratios of monomers change).

The existence of complexes can be ascertained by observing anomalous melting points for mixtures. For example, hexafluorobenzene and benzene melt at 5.2 and 5.5 °C, respectively. Their 1:1 equimolar mixture has an anomalously high melting point of  $\sim 24$  °C. Using DSC, FSt and St monomers were found to have melting points of  $-47 \pm 2$  and  $-30 \pm 1$  °C, respectively. However, melting points for  $\text{N}_3\text{St}$  and 1:1 mixtures of  $\text{N}_3\text{St}$  with FSt and St monomers were not detectable within the lower temperature limit of our instrument ( $-70$  °C). This was confirmed visually by primitive melting point experiments: samples in sealed melting point tubes were placed in a pentane filled bath and allowed to gradually warm. FSt and St monomer melting points were confirmed.  $\text{N}_3\text{St}$  and co-monomer mixtures were found to have melting points below the temperature limit of the precision thermometer ( $-50$  °C). On the basis of the melting point experiments, no co-monomer associations were discernible.

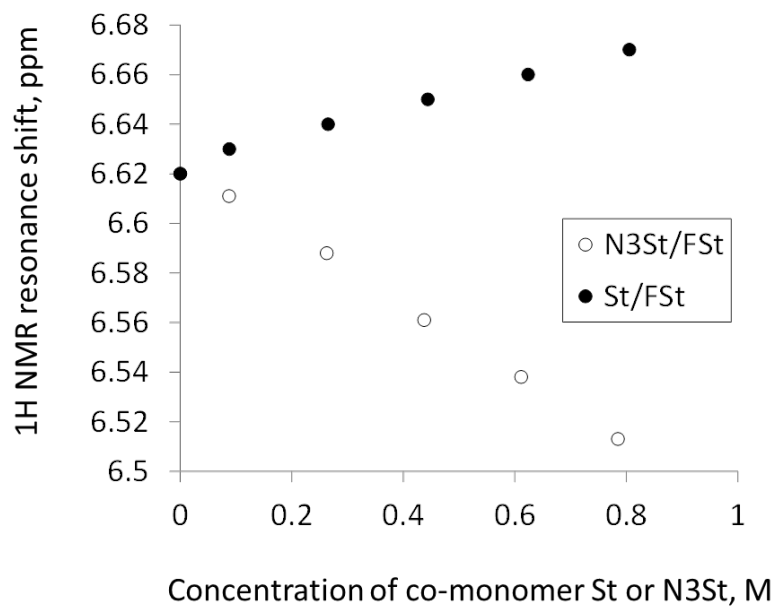
$^1\text{H}$  NMR experiments were used to attempt detection of monomer complexes by resonance shifts of the monomer peaks. At lower concentrations (1 M in  $\text{CDCl}_3$ ) experiments indicated that the resonance peaks of the co-monomer mixtures were shifted. However, the linearity of the shifts suggests that this is due to a solvent effect (S 1, 2, 3).



S 1.  $^1\text{H}$ -NMR resonance shifts of St/FSt co-monomer blends (1 M in  $\text{CDCl}_3$ ).



S 2.  $^1\text{H-NMR}$  resonance shifts of  $\text{N}_3\text{St}/\text{FSt}$  co-monomer blends (1 M in  $\text{CDCl}_3$ ).



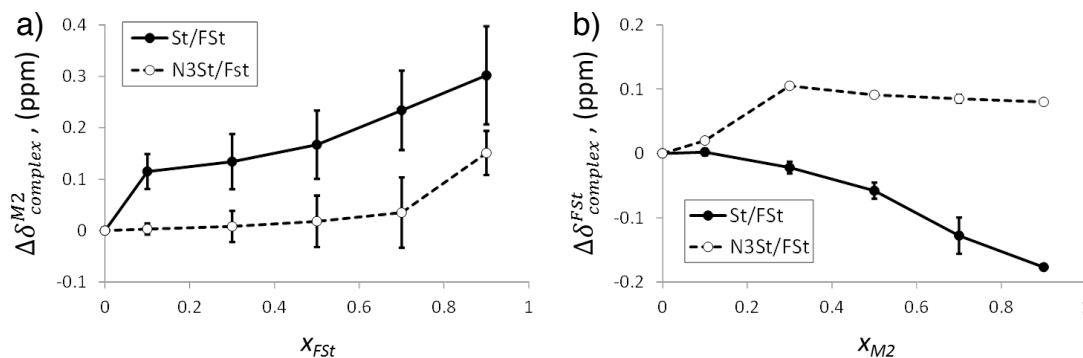
S 3. Comparison of  $^1\text{H-NMR}$  resonance shift of  $-\text{CH}=\text{CH}_2$  proton of co-monomer blends (1 M in  $\text{CDCl}_3$ ).

In this case, it was more informative to use neat mixtures of the monomers as reagents. The chemical shift of vinyl protons (FSt or the second monomer, St or N<sub>3</sub>St) changes significantly and in a non-linear manner varying mole ratio of the neat monomers (25°C, coaxial sample tubes with D<sub>2</sub>O used for NMR lock) indicates formation of the hypothesized complex species (S 4, S 5 and S 6). Attempts at determining the equilibrium concentration using the approach of Hanna and Ashbaugh<sup>7</sup> proved unsuccessful in this case possibly due to the model limitations raised in their paper. The modified Rose-Drago<sup>8</sup> graphical approach described by Wachter and Fried<sup>9</sup> finds the equilibrium constant  $k$  and chemical shift of the pure complex ( $\Delta\delta_C$ ) from the intersection of different  $K_C^{-1}$  versus  $\Delta\delta_C$  traces, where:

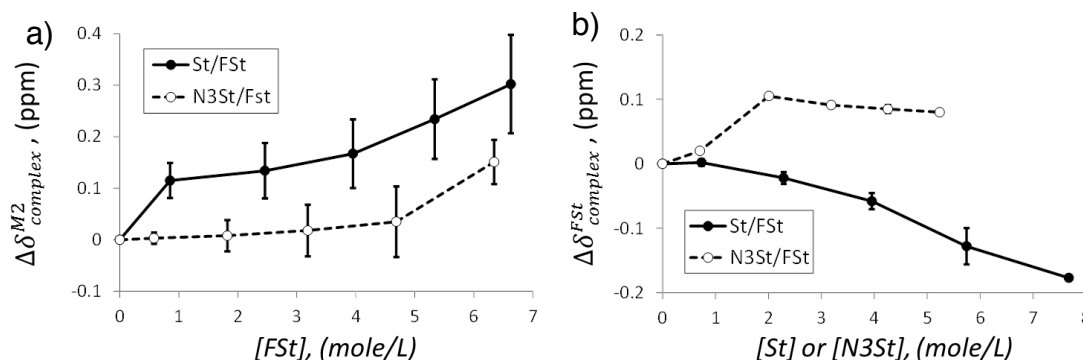
$$K_C^{-1} = \frac{([M_1] \cdot [M_2]) - M_1 \left( \frac{\Delta\delta_{M1}}{\Delta\delta_C} \right) ([M_1] + [M_2]) + [M_1]^2 \left( \frac{\Delta\delta_{M1}}{\Delta\delta_C} \right)^2}{M_1 \left( \frac{\Delta\delta}{\Delta\delta_C} \right)}$$

and  $\Delta\delta_C$  is an assumed range of reasonably expected values ( $C$  refers to the

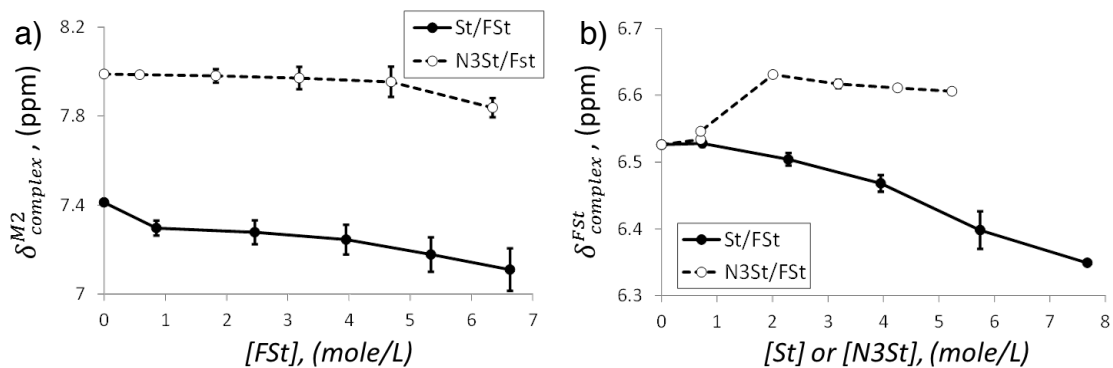
complex and  $M_1$  and  $M_2$  to monomers). A region within which these lines intersect is thereby outlined and the intersection ordinates are averaged to give  $K_C^{-1}$ . Unfortunately we have found that the hyperbolic relation between  $K_C^{-1}$  and  $\Delta\delta_C$  makes the resulting intersection values strongly sensitive to the initial range of  $\Delta\delta_{complex}$  chosen as demonstrated by S 7 for FSt/St monomer mixtures. Assuming  $0 \leq \Delta\delta_C \leq 0.5$ , the  $K_C$  values ranges: 0.08-2.60 ( $K_C^{FSt/St} = 0.2$ ) and 0.24-0.98 ( $K_C^{FSt/N3St} = 0.5$ ) are found respectively for the complexes in neat FSt/St and FSt/N<sub>3</sub>St mixtures. Given the sensitivity of this analysis, these values seem reasonable but are subject to large proportional error in the order of  $\pm 0.5$ .



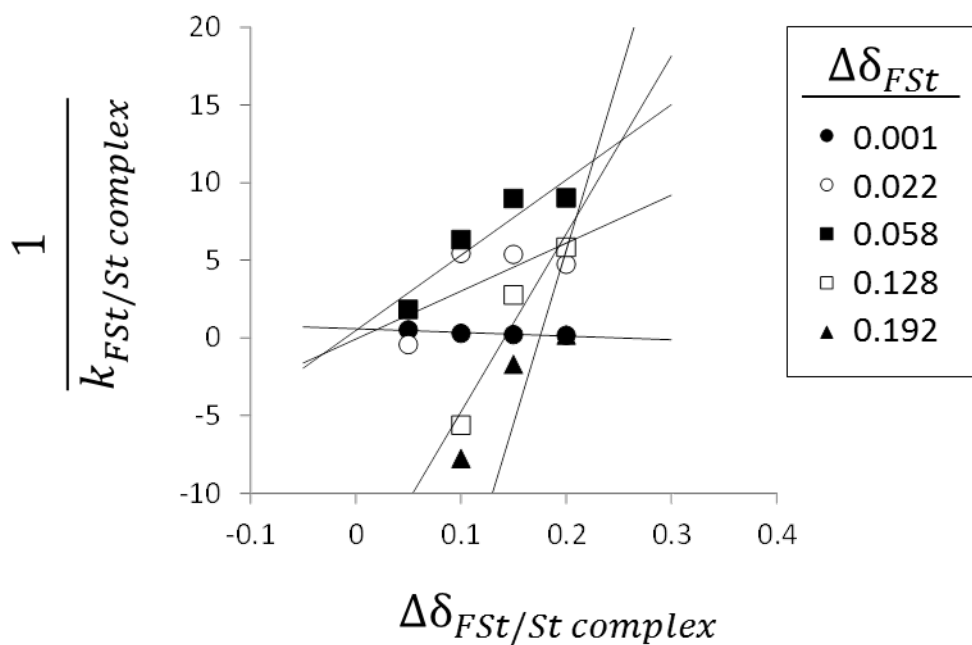
S 4. Change in chemical shift ( $\Delta\delta_{complex}$ ) of FSt or monomer 2 ( $M_2 = St$  or  $N_3St$ ) due to formation of complexes in FSt/ $M_2$  neat mixtures at different monomer ratios (as mole fractions of  $M_2$  or FSt respectively).



S 5. Change in chemical shift ( $\Delta\delta_{complex}$ ) of FSt or monomer 2 ( $M_2 = St$  or  $N_3St$ ) due to formation of complexes in FSt/ $M_2$  neat mixtures at different monomer ratios (as concentration of  $M_2$  or FSt respectively).



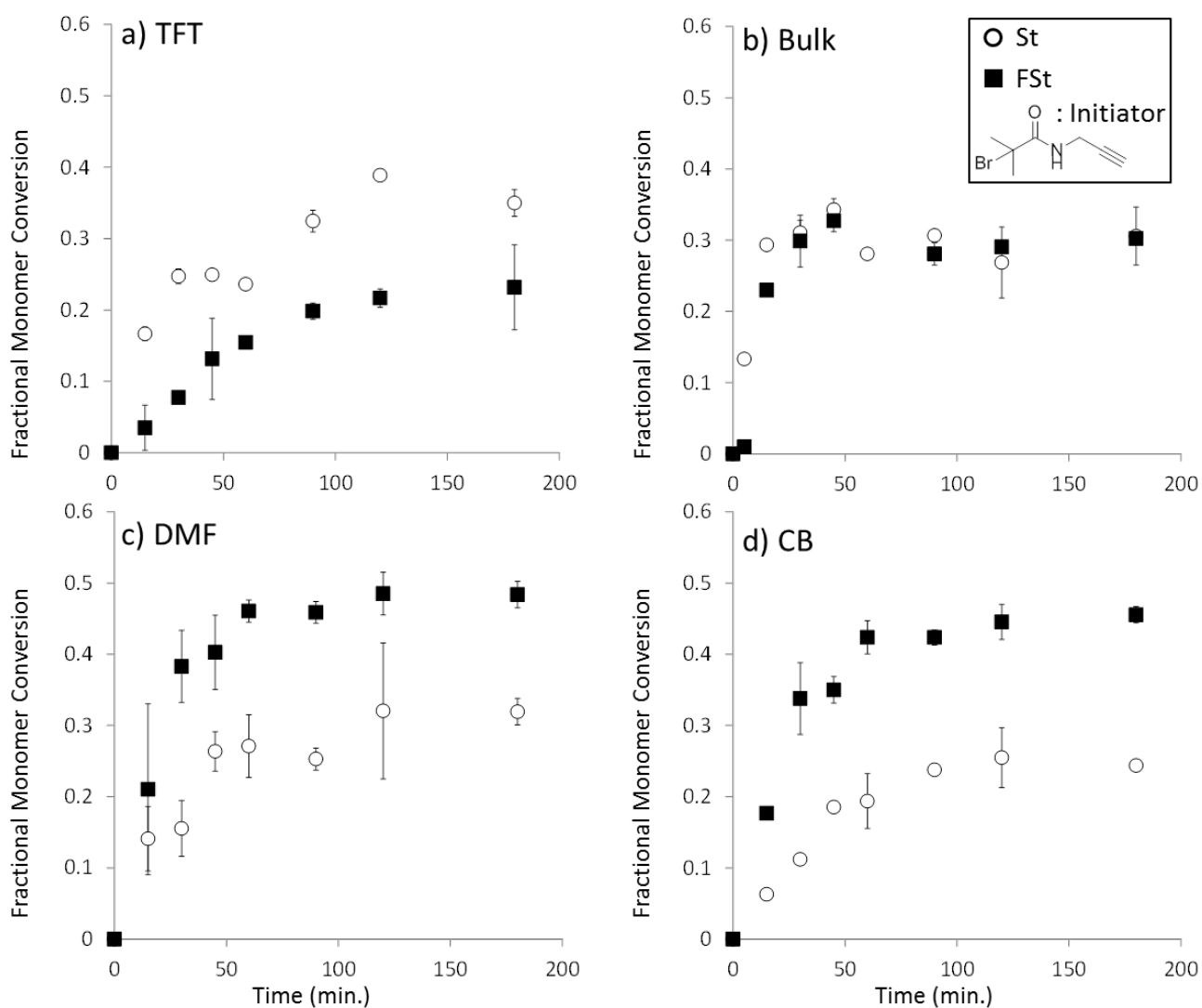
S 6. Chemical shift ( $\delta_{complex}$ ) of FSt or monomer 2 ( $M2 = St$  or  $N_3St$ ) due to formation of complexes in FSt/ $M2$  neat mixtures at different monomer ratios (as concentration of  $M2$  or FSt respectively).



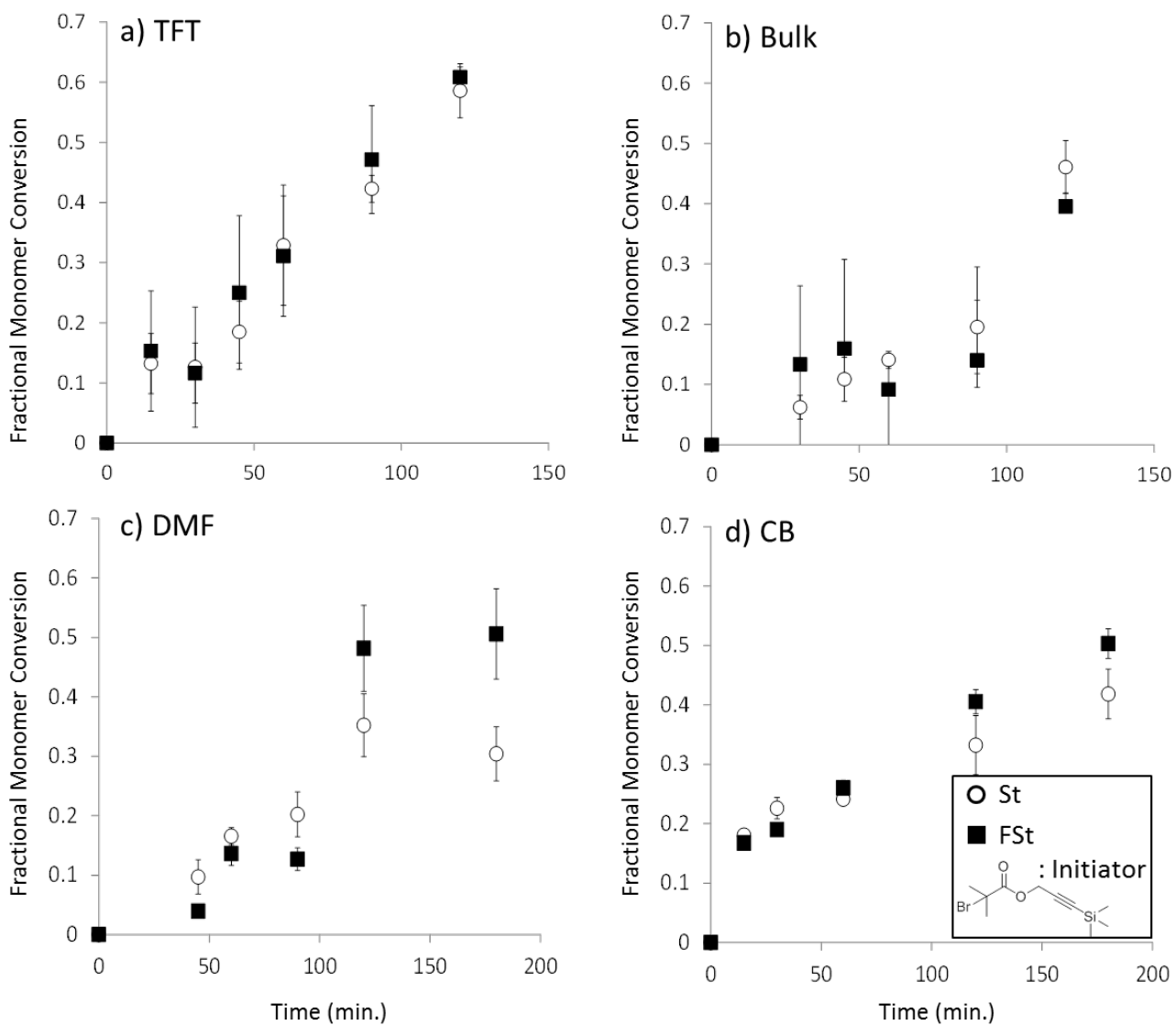
S 7.  $1/K_{complex}$  vs  $\Delta\delta_{complex}$  for different values of experimentally determined  $\Delta\delta_{FSt}$  for determination of  $K_{FSt/St\ complex}$  in FSt/St mixtures.

## 5. General ATRP methods and copolymerization kinetics

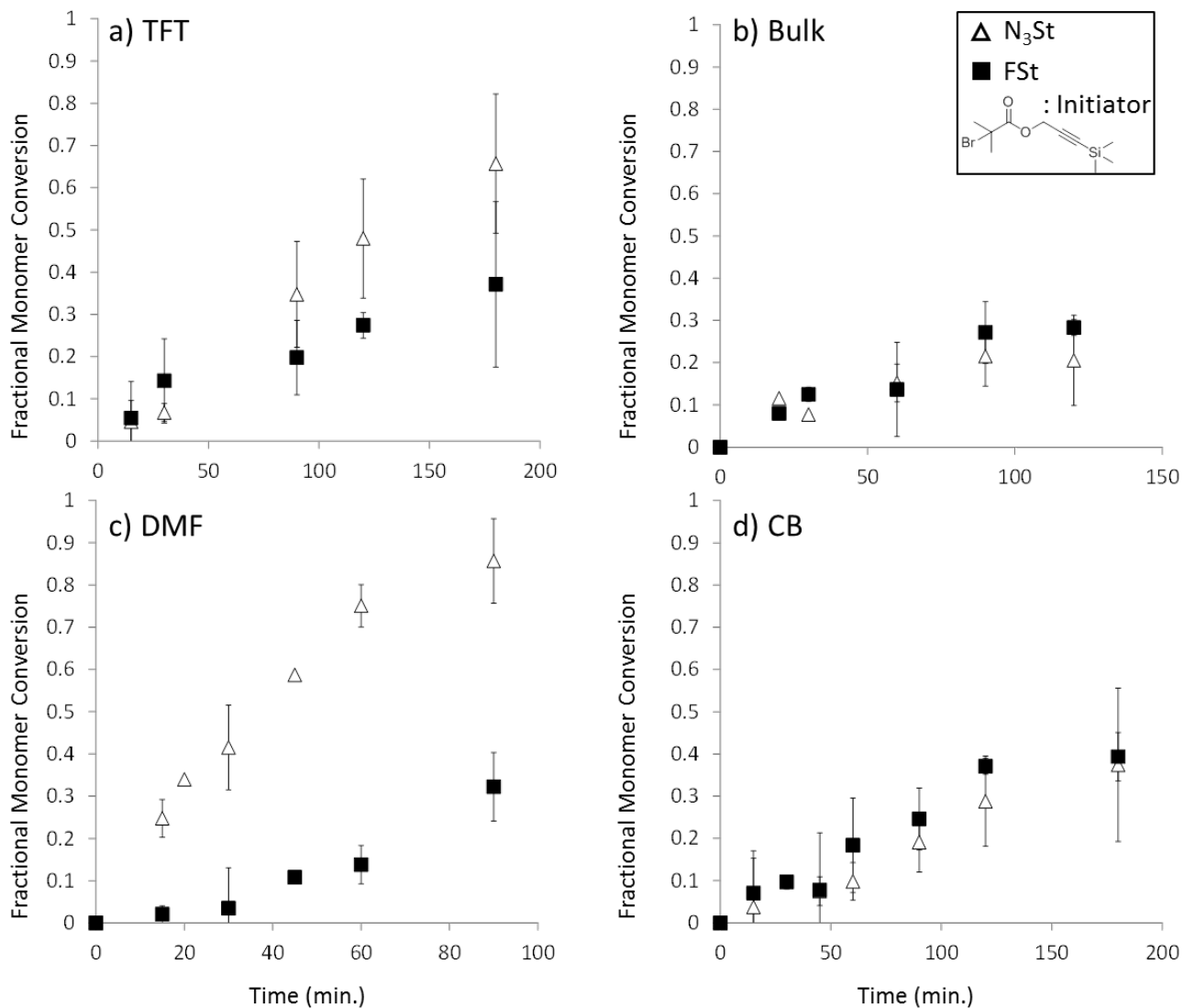
The kinetics of co-polymerizing FSt with either St or N<sub>3</sub>St was studied in different solvents or in bulk using the following ratio of components in the reaction mixture (comonomer : FSt : PMDETA : CuBr : Initiator = 50:50:2:1:1.). In a typical experiment, a 25 mL dried Schlenk flask containing a magnetic stirrer bar was charged with appropriate amounts of monomer; solvent (anhydrous DMF, TFT, CB) if used so that the mixture is 50 % v/v; PMDETA as the ligand; initiator (either PBMP or TPMP); and 100 μL of hexadecane as the internal standard for GCMS analysis. The mixture was degassed by five freeze-pump-thaw cycles. The mixture was again frozen and under nitrogen, CuBr was added and a rubber septum fitted. After several evacuation and N<sub>2</sub> purge cycles of the Schlenk line, the mixture was thawed and an initial sample was taken before placing the flask connected to a continuous N<sub>2</sub> flow in a 90°C oil bath. Subsequently, samples were taken using an N<sub>2</sub> purged needle and syringe, through the rubber septum. Samples were diluted 100-fold with THF and filtered with a 0.45 μm nylon filter before analysis using GCMS and SEC. Samples for NMR analysis were passed through a neutral alumina column before concentration and repeated dissolution/precipitation into MeOH to remove unreacted monomer.



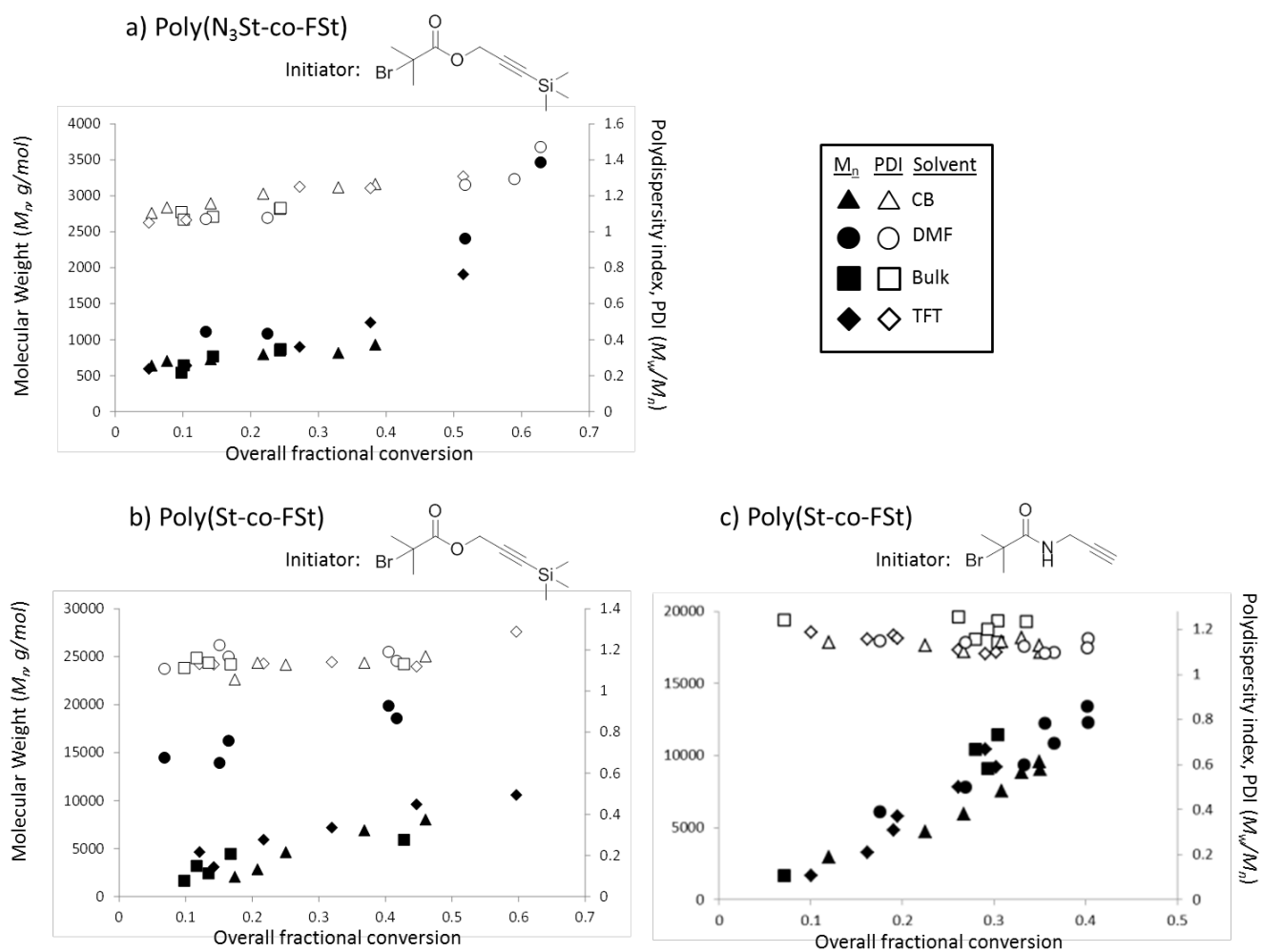
S 8. Copolymerization kinetics of FSt and St under various conditions with ATRP initiator BP. Monomer conversion (GCMS, hexadecane internal standard) with polymerization time in different solvent (50 % v/v, 80°C) and in bulk: a) TFT; b) bulk; c) DMF; d) CB.



**S 9. Copolymerization kinetics of FSt and St under various conditions with ATRP initiator TP. Monomer conversion (GCMS, hexadecane internal standard) with polymerization time in different solvent (50 % v/v, 80°C) and in bulk: a) TFT; b) bulk; c) DMF; d) CB.**



**S 10.** Copolymerization kinetics of N<sub>3</sub>St and FSt under various conditions with ATRP initiator TP. Monomer conversion (GCMS, hexadecane internal standard) with polymerization time in different solvent (50 % v/v, 80°C) and in bulk: a) TFT; b) bulk; c) DMF; d) CB.



S 11. Molecular weight and polydispersity of copolymerization of FSt with N<sub>3</sub>St and St at 80°C under various conditions: a) P(N<sub>3</sub>St-co-FSt) initiated with TP; b) P(St-co-FSt) initiated with TP; c) P(St-co-FSt) initiated with BP.

## 6. Determination of reactivity ratios

Reactivity ratios for the St/FSt and N<sub>3</sub>St/FSt pairs were determined under both controlled (ATRP) and conventional free-radical (FRP) polymerization conditions, where the initiators and solvents were systematically varied. Based on previous work<sup>10-14</sup> in the field, we initially made the assumption that terminal-model kinetics are applicable.<sup>15</sup> The terminal model assumes that reactivity depends solely on the identity of the last reactive monomer group, and is unaffected by composition of the rest of the growing chain.<sup>16</sup> Subsequently, we sought to determine reactivity ratios through a Fineman-Ross graphical solution method to the copolymerization equation.<sup>17</sup> When we compared these values of reactivity ratios in different solvents, we found only a loose correspondence with observed reaction kinetics. While the reaction kinetics indicated wildly variant copolymerization behavior and preferential monomer incorporation depending on the solvent and initiator, the difference in reactivity ratios across these conditions was much smaller than we expected.

Solvent effects were demonstrably prevalent in our study. While influence of solvent can be considerable in some radical reactions, these effects are typically far less subtle than a slight change in differential reactivity between two structurally related monomers.<sup>18</sup> For any given initiator system, our choice of solvent had little impact on the degree of polymerization, or the PDI of the resulting polymers. If the chain-propagation transition state, or any of the side reaction transition states were significantly susceptible to solvent effects, we would expect the opposite outcome.

Therefore, the observed changes in monomer alternation must be attributed to other factors. We have identified the presence of St-FSt monomer complexes by NMR, and it is likely that solvents will strongly affect the formation of these complexes. Our DLS observations support the existence of liquid domains, which may be occurring due to monomer/solvent partitioning. In a previous study, it was concluded that “bad solvents” caused variations in local monomer concentrations, and thus affected co-monomer reactivity.<sup>19</sup> It is reasonable to argue that this monomer pre-arrangement largely determines the final alternation mode.

Taking these considerations into account, we believe that terminal-model kinetics may not be applicable to reactions such as the one under consideration, where monomer complexes play a central role. Consequently, we applied a Karad-Schneider<sup>20</sup> complex-addition model, which modifies the terminal-model by assuming that a 1:1 comonomer complex can add to a propagating radical. In choosing this model, we have assumed that the existence or disruption of co-monomer complexes is related to (and incorporates effects due to) the variations in local monomer concentration, for instance monomer nanodomains. In the rest of this section, we describe the procedures we used to obtain conversions and polymer compositions for subsequent use in the reactivity models described above.

**Reactivity ratios determined from ATRP:** A similar procedure to that followed for the copolymerization kinetics experiments was employed. The reaction mixture (0.25 mL bulk monomer basis) in this case comprised comonomer : FSt : PMDETA : CuBr : Initiator = X:(100-X):2:1:1, where X was equal to 10, 30, 50, 70 or 90 and either 3-(trimethylsilyl)prop-2-yn-1-yl 2-bromo-2-methylpropanoate (TP) or 2-bromo-2-methyl-N-(prop-2-yn-1-yl)propanamide (BP) were used as initiators. Where required, solvent (DMF or TFT) was added (50 % v/v bulk monomer basis). Additionally, dimethoxyethane (0.01 mL) was added as the internal NMR standard. Reaction mixtures were degassed as described and reacted at 80°C for 30 minutes or less, so that a conversion of no greater than 15 % was obtained (bulk monomer basis). The reactions were quenched by dipping the flasks in liquid nitrogen. NMR samples (CDCl<sub>3</sub>) were taken before and after the reaction. The reaction mixture was then diluted with DCM and either extracted with saturated disodium EDTA solution or passed through a column of neutral alumina to remove the copper catalyst. The volume of the solu-

tions was reduced by rotary evaporation. Subsequently, the polymer was precipitated by the addition of MeOH to the reaction mixture and then purified by two further dissolution/re-precipitation cycles. The polymers were dried under vacuum at 50°C overnight, and then characterized by SEC and NMR.

*Reactivity ratios determined from FRP:* The same overall procedure was applied for the FRP experiments except that the reaction mixtures comprised comonomer : FSt : AIBN = X:(100-X):1. The absence of catalyst in this case obviates the necessity for copper removal procedures.

*Determination of monomer conversion:* Comparison of the initial and final <sup>1</sup>H NMR spectra (CDCl<sub>3</sub>) was used to find the monomer conversion with reference to the internal standard dimethoxyethane. The integrals of the vinyl α-hydrogen peaks of FSt (1H, d, 6.1 ppm) and St (1H, d, 5.1 ppm) or N<sub>3</sub>-St (1H, d, 5.3 ppm) were normalized against the integrals of the methyl peaks in 1,2-dimethoxyethane (6H, s, 3.4 ppm). The final conversion (*c<sub>m</sub>*) for a monomer (*m*) is given by  $c_m = 1 - (M_f / M_i)$ ; where *M* is the normalized integral of a particular monomer and; the subscripts *i* and *f* refer to initial and final values respectively. Total monomer conversion (*c<sub>t</sub>*) is given by  $c_t = f_1 c_{m1} + f_2 c_{m2}$  where; *f* is the initial mole fraction of either monomer **1** or **2**.

*Determination of polymer composition:* <sup>1</sup>H NMR spectra (CDCl<sub>3</sub>) of the polymers were used to find the copolymer compositions. The mole fraction of either St or N<sub>3</sub>St in the polymer was found by comparison of the integrals of the five aromatic protons with the three backbone protons. Hence, mole fraction of co-monomer (*F<sub>1</sub>*) is given by  $F_1 = S/B$  where; the normalized integrals of the aromatic protons is  $S = (\text{integral of multiplet between 7.5 and 6.5 ppm})/5$  and the normalized integrals of the backbone protons is  $B = (\text{integral of multiplet between 3.0 and 1.5 ppm})/3$ .

The mole fraction of *F<sub>2</sub>* is given by  $F_2 = 1 - F_1$ .

*Determination of Fineman-Ross reactivity ratios:* The differential copolymer composition (Mayo-Lewis) equation is given by

$$\frac{F_1}{F_2} = \frac{f_1(r_1 f_1 + f_2)}{f_2(r_2 f_2 + f_1)} \quad .^{15}$$

The Fineman-Ross linearization of this equation provides a graphical means of determining the reactivity ratios *r<sub>1</sub>* and *r<sub>2</sub>* by  $G = r_1 F - r_2$  where:  $G = (F_0 - 1)(f_0 / F_0)$ ;  $H = f_0^2 / F_0$ ;  $f_0 = f_1 / f_2$ ;  $F_0 = F_1 / F_2$ ; and, *f* and *F* are respectively the mole fractions of the monomers initially and in the polymer.<sup>17</sup> Finding the variation in polymer composition, *F* for a range of different initial mole fractions, *f* allows calculation and graphical representation of *G* and *H*. Linear regression of the data gives a line where the slope is *r<sub>1</sub>* and the intercept is *r<sub>2</sub>*.

**Table 2. Reactivity ratio data.**

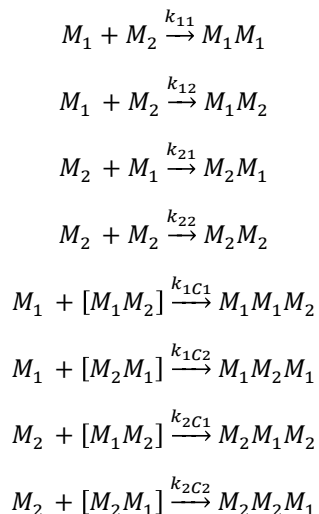
Entry #	$M_1^a$	Initiator	Solvent	$f_1^b$	$F_1^c$	$F_2^d$	$M_n \times 10^{-3}$	$PDI$	$f_0^e$	$F_0^f$	$H^g$	$G^h$	$r_1^i$	$r_2^j$	$r_1 \cdot r_2$
1	St	TP	bulk	0.1	0.26	0.74	6.30	1.10	0.11	0.35	0.04	-0.21			
2	St	TP	bulk	0.3	0.40	0.60	5.87	1.11	0.43	0.66	0.28	-0.23			
3	St	TP	bulk	0.5	0.50	0.50	8.75	1.13	1.00	0.99	1.01	-0.01	0.181	0.186	0.034
4	St	TP	bulk	0.7	0.58	0.42	2.10	1.12	2.33	1.39	3.91	0.66			
5	St	TP	bulk	0.9	0.72	0.28	2.38	1.13	9.00	2.57	31.50	5.50			
6	St	TP	DMF	0.1	0.14	0.86	9.00	1.08	0.11	0.16	0.08	-0.58			
7	St	TP	DMF	0.3	0.29	0.71	42.7	1.18	0.43	0.42	0.44	-0.60			
8	St	TP	DMF	0.5	0.39	0.61	18.4	1.13	1.00	0.64	1.56	-0.56	0.061	0.872	0.053
9	St	TP	DMF	0.7	0.40	0.60	9.23	1.08	2.33	0.66	8.30	-1.23			
10	St	TP	DMF	0.9	0.59	0.41	5.39	1.09	9.00	1.43	56.76	2.69			
11	St	TP	TFT	0.1	0.23	0.77	22.6	1.10	0.11	0.31	0.04	-0.25			
12	St	TP	TFT	0.3	0.34	0.66	15.8	1.18	0.43	0.51	0.36	-0.42			
13	St	TP	TFT	0.5	0.48	0.52	1.53	1.11	1.00	0.92	1.08	-0.08	0.162	0.334	0.054
14	St	TP	TFT	0.7	0.55	0.45	8.71	1.15	2.33	1.20	4.53	0.39			
15	St	TP	TFT	0.9	0.42	0.58	1.12	1.12	9.00	0.73	110.70	-3.30			
16	St	AIBN	DMF	0.1	0.30	0.70	33.2	1.30	0.11	0.42	0.03	-0.15			
17	St	AIBN	DMF	0.3	0.16	0.84	29.2	1.25	0.43	0.19	0.95	-1.79			
18	St	AIBN	DMF	0.5	0.42	0.58	27.7	1.33	1.00	0.72	1.38	-0.38	0.222	0.867	0.193
19	St	AIBN	DMF	0.7	0.55	0.45	19.1	1.51	2.33	1.20	4.53	0.39			
20	St	AIBN	DMF	0.9	0.73	0.27	10.8	1.53	9.00	2.73	29.66	5.70			
21	St	AIBN	TFT	0.1	0.20	0.80	17.2	1.48	0.11	0.26	0.05	-0.32			
22	St	AIBN	TFT	0.3	0.34	0.66	23.2	1.49	0.43	0.51	0.36	-0.42			
23	St	AIBN	TFT	0.5	0.47	0.53	23.5	1.40	1.00	0.90	1.11	-0.11	0.099	0.231	0.023
24	St	AIBN	TFT	0.7	0.56	0.44	19.0	1.45	2.33	1.29	4.21	0.53			
25	St	AIBN	TFT	0.9	0.65	0.35	14.5	1.31	9.00	1.84	44.00	4.11			
26	N <sub>3</sub> St	AIBN	bulk	0.1	0.22	0.78	34.3	1.77	0.11	0.29	0.04	-0.27			
27	N <sub>3</sub> St	AIBN	bulk	0.3	0.58	0.42	27.6	1.76	0.43	1.36	0.14	0.11			
28	N <sub>3</sub> St	AIBN	bulk	0.5	0.46	0.54	22.4	1.61	1.00	0.86	1.16	-0.16	0.756	0.433	0.327
29	N <sub>3</sub> St	AIBN	bulk	0.7	0.70	0.30	12.0	1.37	2.33	2.31	2.36	1.32			
30	N <sub>3</sub> St	AIBN	bulk	0.9	0.88	0.12	11.6	1.30	9.00	7.50	10.80	7.80			
31	N <sub>3</sub> St	AIBN	DMF	0.1	0.14	0.86	32.2	1.60	0.11	0.17	0.07	-0.55			
32	N <sub>3</sub> St	AIBN	DMF	0.3	0.24	0.76	28.5	1.65	0.43	0.31	0.59	-0.96			
33	N <sub>3</sub> St	AIBN	DMF	0.5	0.31	0.69	21.2	1.68	1.00	0.45	2.23	-1.23	0.086	0.935	0.080
34	N <sub>3</sub> St	AIBN	DMF	0.7	0.48	0.52	16.9	1.52	2.33	0.91	5.99	-0.23			
35	N <sub>3</sub> St	AIBN	DMF	0.9	0.49	0.51	11.4	1.55	9.00	0.97	83.70	-0.30			
36	N <sub>3</sub> St	AIBN	TFT	0.1	0.19	0.81	23.6	1.46	0.11	0.24	0.05	-0.36			
37	N <sub>3</sub> St	AIBN	TFT	0.3	0.31	0.69	20.6	1.51	0.43	0.45	0.41	-0.52	0.348	0.486	0.169
38	N <sub>3</sub> St	AIBN	TFT	0.5	0.49	0.51	17.5	1.54	1.00	0.95	1.06	-0.06			

39	N <sub>3</sub> St	AIBN	TFT	0.7	0.43	0.57	13.5	1.35	2.33	0.76	7.17	-0.74			
40	N <sub>3</sub> St	AIBN	TFT	0.9	0.48	0.52	10.3	1.24	9.00	0.91	89.10	-0.90			
1	N <sub>3</sub> St	TP	DMF	0.1	0.14	0.86	2.44	1.13	0.11	0.17	0.07	-0.56			
2	N <sub>3</sub> St	TP	DMF	0.3	0.36	0.64	2.25	1.19	0.43	0.56	0.33	-0.33			
3	N <sub>3</sub> St	TP	DMF	0.5	0.52	0.48	1.96	1.16	1.00	1.06	0.94	0.06	1.527	1.107	1.691
4	N <sub>3</sub> St	TP	DMF	0.7	0.72	0.28	1.22	1.17	2.33	2.56	2.13	1.42			
5	N <sub>3</sub> St	TP	DMF	0.9	0.93	0.07	7.50	1.20	9.00	13.50	6.00	8.33			
6	N <sub>3</sub> St	TP	TFT	0.1	0.14	0.86	3.79	1.14	0.11	0.16	0.08	-0.58			
7	N <sub>3</sub> St	TP	TFT	0.3	0.33	0.67	1.46	1.21	0.43	0.50	0.37	-0.43			
8	N <sub>3</sub> St	TP	TFT	0.5	0.46	0.54	1.66	1.23	1.00	0.86	1.16	-0.16	0.609	0.796	0.484
9	N <sub>3</sub> St	TP	TFT	0.7	0.62	0.38	1.41	1.25	2.33	1.64	3.32	0.91			
10	N <sub>3</sub> St	TP	TFT	0.9	0.86	0.14	1.13	1.25	9.00	6.00	13.50	7.50			
7x	N <sub>3</sub> St	TP	bulk	0.1	0.15	0.85	9.20	1.29	9.00	5.47	14.82	7.35			
8x	N <sub>3</sub> St	TP	bulk	0.3	0.33	0.67	3.80	1.28	2.33	0.50	10.89	-2.33			
9x	N <sub>3</sub> St	TP	bulk	0.5	0.48	0.52	2.21	1.26	1.00	0.93	1.08	-0.08	0.286	0.502	0.143
10x	N <sub>3</sub> St	TP	bulk	0.7	0.60	0.40	1.34	1.30	0.43	1.50	0.12	0.14			
11x	N <sub>3</sub> St	TP	bulk	0.9	0.89	0.11	1.17	1.18	0.11	7.80	0.00	0.10			
1	St	BP	DMF	0.1	0.16	0.84	9.18	1.10	9.00	5.30	15.28	7.30			
2	St	BP	DMF	0.3	0.33	0.67	7.69	1.12	2.33	0.49	11.05	-2.40			
3	St	BP	DMF	0.5	0.42	0.58	4.55	1.13	1.00	0.72	1.39	-0.39	0.303	0.853	0.258
4	St	BP	DMF	0.7	0.46	0.54	2.29	1.15	0.43	0.85	0.22	-0.08			
5	St	BP	DMF	0.9	0.25	0.75	1.45	1.23	0.11	0.34	0.04	-0.22			
6	St	BP	TFT	0.1	0.22	0.78	2.00	1.18	0.11	0.27	0.05	-0.29			
7	St	BP	TFT	0.3	0.48	0.52	3.37	1.15	0.43	0.92	0.20	-0.04			
8	St	BP	TFT	0.5	0.76	0.24	1.51	1.16	1.00	3.16	0.32	0.68	0.931	0.076	0.071
9	St	BP	TFT	0.7	0.75	0.25	1.30	1.16	2.33	3.00	1.81	1.56			
10	St	BP	TFT	0.9	0.84	0.16	6.80	1.17	9.00	5.36	15.12	7.32			
1	St	BP	bulk	0.1	0.40	0.60	6.40	1.17	0.11	0.66	0.02	-0.06			
2	St	BP	bulk	0.3	0.41	0.59	6.30	1.28	0.43	0.68	0.27	-0.20			
3	St	BP	bulk	0.5	0.48	0.52	4.14	1.17	1.00	0.92	1.09	-0.09	0.243	0.213	0.052
4	St	BP	bulk	0.7	0.59	0.41	6.00	1.16	2.33	1.46	3.72	0.74			
5	St	BP	bulk	0.9	0.52	0.48	1.30	1.16	9.00	1.06	76.27	0.53			

<sup>a</sup> Co-monomer with FSt; <sup>b</sup> Initial mole fraction co-monomer  $M_1$ ; <sup>c</sup> Mole fraction of co-monomer in resulting polymer; <sup>d</sup> Mole fraction of FSt in resulting polymer; <sup>e</sup> Initial mole ratio of monomers ( $f_0 = f_1/f_2$ ); <sup>f</sup> Mole ratio of monomers in resulting polymer ( $F_0 = F_1/F_2$ ); <sup>g</sup> Ordinate on the horizontal axis from Fineman-Ross linearization of copolymer equation ( $H = f_0^2/F_0$ ); <sup>h</sup> Ordinate on the vertical axis from Fineman-Ross linearization of copolymer equation ( $G = (F_0 - 1) \cdot (f_0/F_0)$ ); <sup>i</sup> Co-monomer reactivity ratio ( $r_1$ ) representing the slope from Fineman-Ross linearization; <sup>j</sup> FSt reactivity ratio ( $r_{12}$ ) representing the negative intercept on the vertical axis from Fineman-Ross linearization.

**Determination of reactivity ratios with complex contribution (Karad-Schneider):** Seiner and Litt considered the influence of weak charge-transfer co-monomer complexes (low complex equilibrium constants ( $0.03 \gg K_C$ ), in free-radical copolymerization.<sup>21</sup> In their treatment, Karad and Schneider extended this to consider the effect of stronger co-monomer complexes ( $0.03 \ll K_C$ ).<sup>20</sup> The

complex  $C \equiv M_1M_2$  may be added to a propagating radical as a distinct unit from the individual monomers, resulting in additional reaction equations:



With: monomer ( $M_i$ ), radical ( $\square$ ), rate constant ( $k_{ij}$ ), complex orientation 1 ( $C1 \equiv M_1M_2$ ), complex orientation 2 ( $C2 \equiv M_2M_1$ ).

So that:

$$r_{12} = \frac{k_{11}}{k_{12}}; \quad r_{1C1} = \frac{k_{11}}{k_{1C1}}; \quad r_{1C2} = \frac{k_{11}}{k_{1C2}}; \quad r_{1C} = \frac{k_{11}}{k_{1C}} \quad \text{with} \quad k_{1C} = k_{1C1} + k_{1C2}$$

Assuming:  $k_{22} = 0$  and  $k_{2C2} = 0$ .

Concentration of the complex  $[C] \equiv [M_1M_2]$  is related to the equilibrium constant of the complex by:

$$K_C = \frac{[C]}{[M_1 - C][M_2 - C]}$$

Which can be solved for  $[C]$ :

$$[C] = \frac{1}{2} \left( [M_1^0] + [M_2^0] + \frac{1}{(K_C)} \right) - \frac{1}{2} \left( ([M_1^0] - [M_2^0])^2 + \frac{2([M_1^0] + [M_2^0])}{(K_C)} + \frac{1}{(K_C)^2} \right)^{1/2}$$

Where,  $[M_i^0] = \text{initial } [M_i]$ .

A linear form of the equation that takes account of this concentration is given as:

$$(F_0 - 1) = \frac{r_{1C}}{r_{1C1}} + r_{1C} \left( \frac{[M_1]}{[C]} - \frac{(F_0 - 1)[M_2]}{r_{12}[C]} \right) \text{ where, } F_0 = F_1/F_2.$$

A graph of  $(F_0 - 1)$  versus  $\left( \frac{[M_1]}{[C]} - \frac{(F_0 - 1)[M_2]}{r_{12}[C]} \right)$  yields  $r_{1C}$  from the slope directly,  $r_{1C1}$  from  $\frac{r_{1C}}{(r_{1C}/r_{1C1})}$  (ie. slope (S) divided by intercept (I)) and  $r_{1C2} = \left( \frac{1}{r_{1C}} - \frac{1}{r_{1C1}} \right)^{-1}$  (ie.  $r_{1C2} = \left( \frac{S}{1-I} \right)$ ).

Initial  $r_{12}$  values can be taken from the Fineman-Ross analysis and then optimized within acceptable limits such that the sum of squares of the linearization is maximized. Limits depend on the level of significance placed on  $r_{1C1}$  and  $r_{1C2}$  as opposed to the less sensitive  $r_{1C}$ . The values of these specific monomer-complex reactivity ratios are very sensitive to subtle numerical variations. Moreover, if  $r_{12}$  is chosen such that the intercept  $r_{1C}/r_{1C1} > 1$ , then  $r_{1C2} < 0$ . Likewise, for  $r_{1C}/r_{1C1} \leq 0$  then  $r_{1C1} < 0$  (assuming that the slope had a positive a gradient). Therefore, choices of  $r_{12}$  are limited by the restriction  $0 \leq r_{1C}/r_{1C1} \leq 1$ . Additionally, Karad and Schneider derived a solution for the relationship:

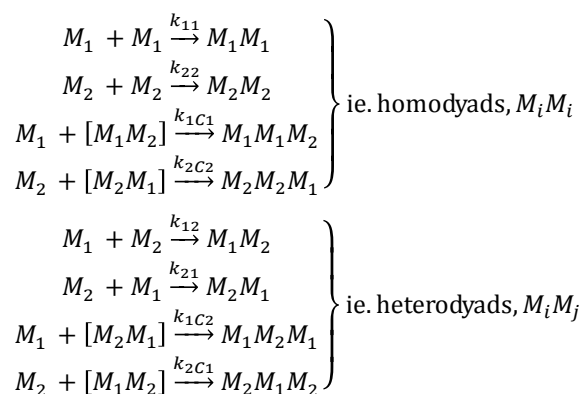
$$r_3 = \frac{r_{21}}{r_{2C1}} = \frac{k_{2C1}}{k_{21}}$$

Similar to Karad and Schneider however, we found that the values thus obtained for  $r_3$  were not informative.

Fineman-Ross reactivity ratios for St/FSt and N<sub>3</sub>St/FSt comonomer pairs found in this study are compared to those reported in literature (Table 3). Strictly, the  $K_C$  values should only be applied to polymerizations conducted under the same conditions in which the equilibrium constants were determined (bulk, 25°C). At higher temperatures and/or in solvent  $K_C$  will decrease by at least an order of magnitude, and hence the values determined for  $r_{1C}$  will similarly vary. However, for the purposes of gauging the contribution of complex participation during polymerization, Karad-Schneider monomer-complex reactivity ratios have been calculated both for this study and from published data sets for which only Fineman-Ross calculations had previously been reported.

Inspection of Table 3 reveals that based on Fineman-Ross reactivity ratios and cross products, alternation between co-monomers should be expected during polymerization under most of the temperature and solvent conditions presented ( $r_{ij} < 1$ ). A notable exception is the ATRP of N<sub>3</sub>St/FSt in DMF. In contrast, the kinetic results indicate significant monomer selectivity occurring, which seemingly depends on the particular co-monomer, solvent and initiator combinations employed. The variation of the Fineman-Ross reactivity ratios across these combinations qualitatively agrees with the changes in reactivity seen in the kinetics results.

It is instructive to consider the overall propensity for a system to result in homo- or hetero- dyads. Since we have assumed that the complex reacts as a discrete unit, to determine the ratio of homo- to cross- propagation, a facile treatment is required to reconcile the occurrence of homo-dyads  $M_iM_i$  with occurrence of the hetero-dyads  $M_iM_j$  via the alternate pathways:



Under the specific circumstances that  $k_{22} = k_{2C2} = 0$  (i.e. FSt does not homopolymerize) and  $k_{21} \approx k_{2C1} \ll k_{12}$  the ratio of the rate constants of the reactions resulting in homo- to hetero- dyads becomes  $r_4$ :

$$r_4 = \frac{k_{11} + k_{1C1}}{k_{12} + k_{1C2}}$$

Hence,

$$\frac{k_{11} + k_{1C1}}{k_{12} + k_{1C2}} = \frac{k_{11}}{k_{12} + k_{1C2}} + \frac{k_{1C1}}{k_{12} + k_{1C2}}$$

with the first term,

$$\frac{k_{11}}{k_{12} + k_{1C2}} = \left[ \frac{k_{12} + k_{1C2}}{k_{11}} \right]^{-1} = \left[ \frac{k_{12}}{k_{11}} + \frac{k_{1C2}}{k_{11}} \right]^{-1} = \left[ \frac{1}{r_{12}} + \frac{1}{r_{1C2}} \right]^{-1}$$

and the second term,

$$\frac{k_{1C1}}{k_{12} + k_{1C2}} = \left[ \frac{k_{12} + k_{1C2}}{k_{1C1}} \right]^{-1} = \left[ \frac{k_{12}}{k_{1C1}} + \frac{k_{1C2}}{k_{1C1}} \right]^{-1} = \left[ \frac{r_{1C1}}{r_{12}} + \frac{r_{1C1}}{r_{1C2}} \right]^{-1}$$

so that combining terms,

$$r_4 = \frac{k_{11} + k_{1C1}}{k_{12} + k_{1C2}} = \left[ \frac{1}{r_{12}} + \frac{1}{r_{1C2}} \right]^{-1} + \left[ \frac{r_{1C1}}{r_{12}} + \frac{r_{1C1}}{r_{1C2}} \right]^{-1}$$

It is clear that the derivation of  $r_4$  is of little value for instances where the assumptions involved ( $k_{22} = k_{2C2} = 0$  and  $k_{21} \approx k_{2C1} \ll k_{12}$ ) are not valid. Specifically,  $r_4$  entries 15-20 in Table 3 (cf. plots c and d in S 8) are of little meaning and included only for comparison, since significant homo-polymerization of FSt occurs in these cases.

**Table 3. Comparison of reactivity ratios determined of FSt ( $M_2$ ) with St or N<sub>3</sub>St ( $M_1$ ) from this study and literature.**

Entry #	$M_1$	T (°C)	Solvent / $\epsilon_{20^\circ C}^a$		Initiator /system	Fineman-Ross <sup>17</sup>				Karad-Schneider <sup>20</sup>			$r_4$	ref.
						$r_1$	$r_2$	$r_1 \cdot r_2$	$K_C^d$	$r_{1C}$	$r_{1C1}$	$r_{1C2}$		
1	N <sub>3</sub> St	80	bulk	/ 2.01 <sup>b</sup>	AIBN / FRP	0.76	0.43	0.327	0.5	0.021	0.118	0.026	0.24	<i>e</i>
2	N <sub>3</sub> St	80	bulk	/ 2.01	TP / ATRP	0.50	0.29	0.143	0.5	0.052	0.150	0.080	0.46	<i>e</i>
3	N <sub>3</sub> St	80	TFT	9.18 <sup>c</sup>	AIBN / FRP	0.35	0.49	0.169	0.5	0.092	0.172	0.197	1.03	<i>e</i>
4	N <sub>3</sub> St	80	TFT	/ 9.18	TP / ATRP	0.61	0.80	0.484	0.5	0.352	0.253	0.893	1.40	<i>e</i>
5	N <sub>3</sub> St	80	DMF	/ 36.7 <sup>c</sup>	AIBN / FRP	0.94	0.09	0.080	0.5	0.055	0.111	0.107	0.82	<i>e</i>
6	N <sub>3</sub> St	80	DMF	/ 36.7	TP / ATRP	1.53	1.11	1.691	0.5	0.168	0.375	0.233	1.3	<i>e</i>
7	St	60	bulk	/ 2.01 <sup>b</sup>	AIBN / FRP	0.43	0.22	0.095	0.2	0.358 <sup>n</sup>	5.54	<i>f</i>	<i>f</i>	11
8	St	25	bulk	/ 2.01	t-BP / FRP	0.22	0.22	0.048	0.2	<i>f, g</i>	<i>f</i>	<i>f</i>	<i>f</i>	13
9	St	70	bulk	/ 2.01	BPO / FRP	0.62	0.28	0.17	0.2	0.129 <sup>n</sup>	0.020	<i>f</i>	<i>f</i>	13
10	St	80	bulk	/ 2.01	BP / ATRP	0.24	0.21	0.052	0.2	0.002	0.0008	0.0015	0.89	<i>e</i>
11	St	80	bulk	/ 2.01	TP / ATRP	0.18	0.18	0.034	0.2	0.280	0.095	0.144	0.37	<i>e</i>
12	St	70	Toluene	/ 2.38 <sup>c</sup>	BPO / FRP	0.47	0.3	0.14	—	—	—	—	—	2
13	St	25	Toluene	/ 2.38	BPO-DMA / Redox	0.3	0.23	0.069	—	—	—	—	—	12
14	St	25	THF	/ 7.6 <sup>c</sup>	n-C <sub>4</sub> H <sub>9</sub> Li / Anionic	0.33	0.43	0.14	—	—	—	—	—	10
15	St	80	DMF	/ 36.7 <sup>c</sup>	AIBN / FRP	0.22	0.87	0.193	0.2	0.027	0.117	0.035	0.29	<i>e</i>
16	St	80	DMF	/ 36.7	BP / ATRP	0.52	0.65	0.340	0.2	0.892	0.280	0.408	0.48	<i>e</i>
17	St	80	DMF	/ 36.7	TP / ATRP	0.06	0.87	0.054	0.2	0.289	0.071	0.095	0.35	<i>e</i>
18	St	80	TFT	/ 9.18 <sup>c</sup>	AIBN / FRP	0.10	0.23	0.023	0.2	0.344	0.018	0.019	0.06	<i>e</i>
19	St	80	TFT	/ 9.18	BP / ATRP	0.93	0.07	0.054	0.2	0.447	0.072	0.086	0.25	<i>e</i>
20	St	80	TFT	/ 9.18 <sup>c</sup>	TP / ATRP	0.16	0.33	0.546	0.2	0.290	0.071	0.095	0.33	<i>e</i>

<sup>a</sup> Dielectric constant; <sup>b</sup> Calculated from reference<sup>22</sup>; <sup>c</sup> From reference<sup>23</sup>; <sup>d</sup> determined in bulk at 25°C; <sup>e</sup> current study; <sup>f</sup> Feasible values cannot be calculated; <sup>g</sup> values are calculated from data provided in referenced literature for comparison;

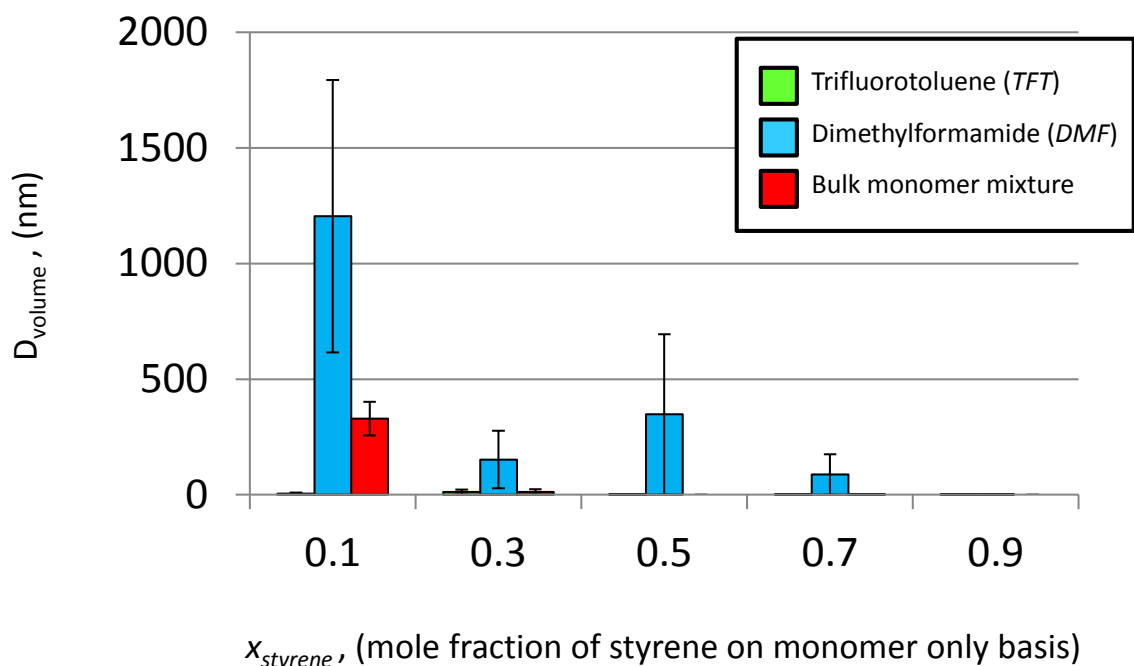
## 7. Identification of liquid domains by DLS

Pentafluorostyrene and styrene mixtures were prepared at different mole fractions of styrene in either bulk, or as solutions in TFT or DMF (50 % v/v with respect to total monomer volume). The samples were filtered through 0.45 micron PTFE syringe filters. The samples and the instrument were equilibrated at 20°C. The instrumental parameters used for the measurements (refractive indices, viscosities and dielectric constants) were based on the literature values at 20°C. Where a literature value could not be found, the value for a similar compound was substituted i.e. hexafluorobenzene for pentafluorostyrene (Table 4). Two repeats were made, and the volume-average diameters are reported.

**Table 4. Property values used for DLS experiments.**

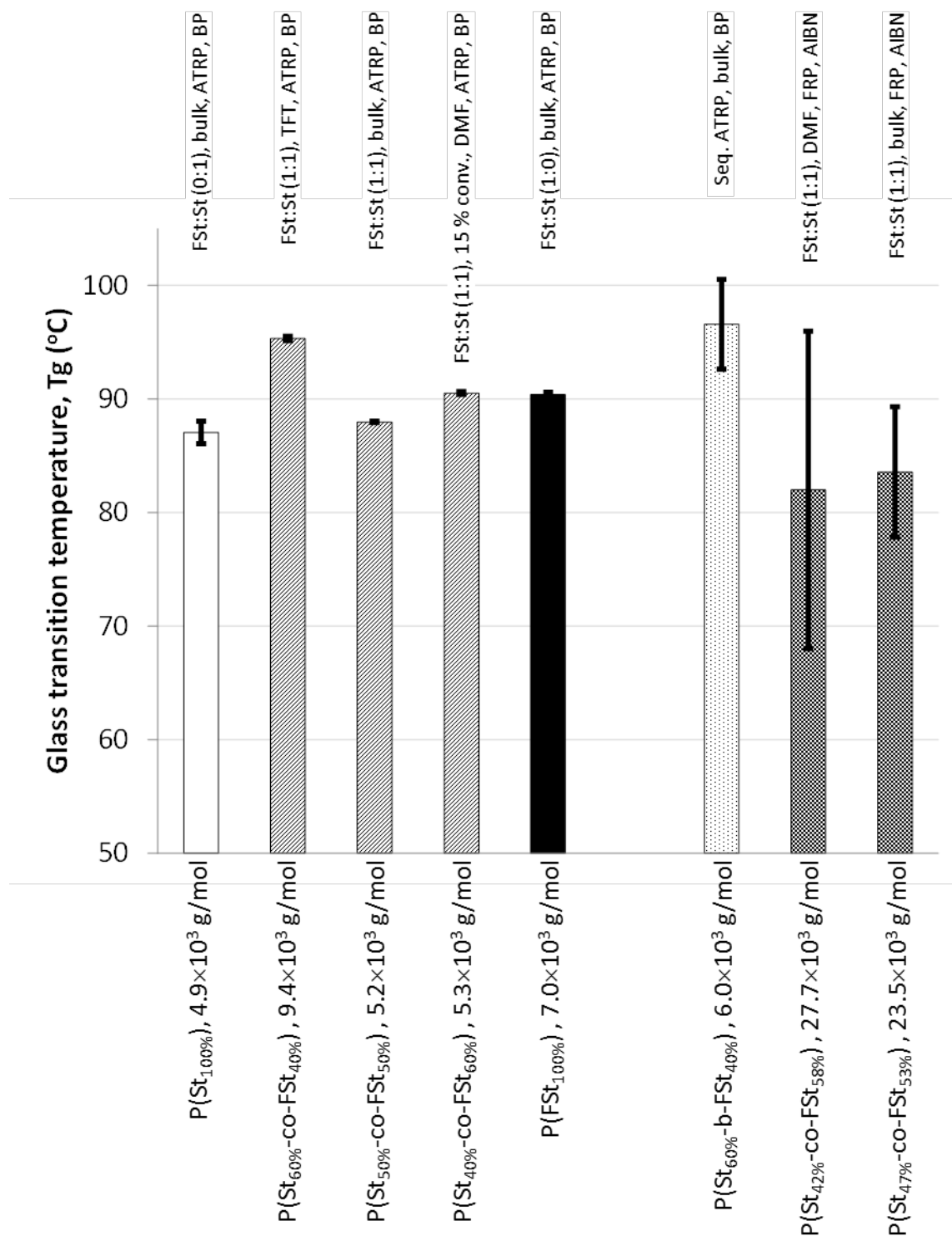
Component	Refractive Index ( $n_{20^{\circ}\text{C}}$ )	Viscosity ( $\eta_{20^{\circ}\text{C}}$ , mPa.s)	Dielectric Constant ( $\epsilon_{20^{\circ}\text{C}}$ )
hexafluorobenzene	1.377 <sup>a</sup>	0.951 <sup>23</sup>	2.015 <sup>23</sup>
trifluorotoluene	1.411 <sup>a</sup>	0.39 <sup>24</sup>	9.22
styrene	1.5445 <sup>b</sup>	0.76 <sup>b</sup>	2.4257 <sup>c</sup>
N, N'-dimethylformamide	1.43058 <sup>23</sup>	0.8668 <sup>23</sup>	37.73 <sup>23</sup>

<sup>a</sup> Manufacturer information (Sigma-Aldrich); <sup>b</sup> Manufacturer information (Sabic); <sup>c</sup> Manufacturer information (Ineos Styrenics).



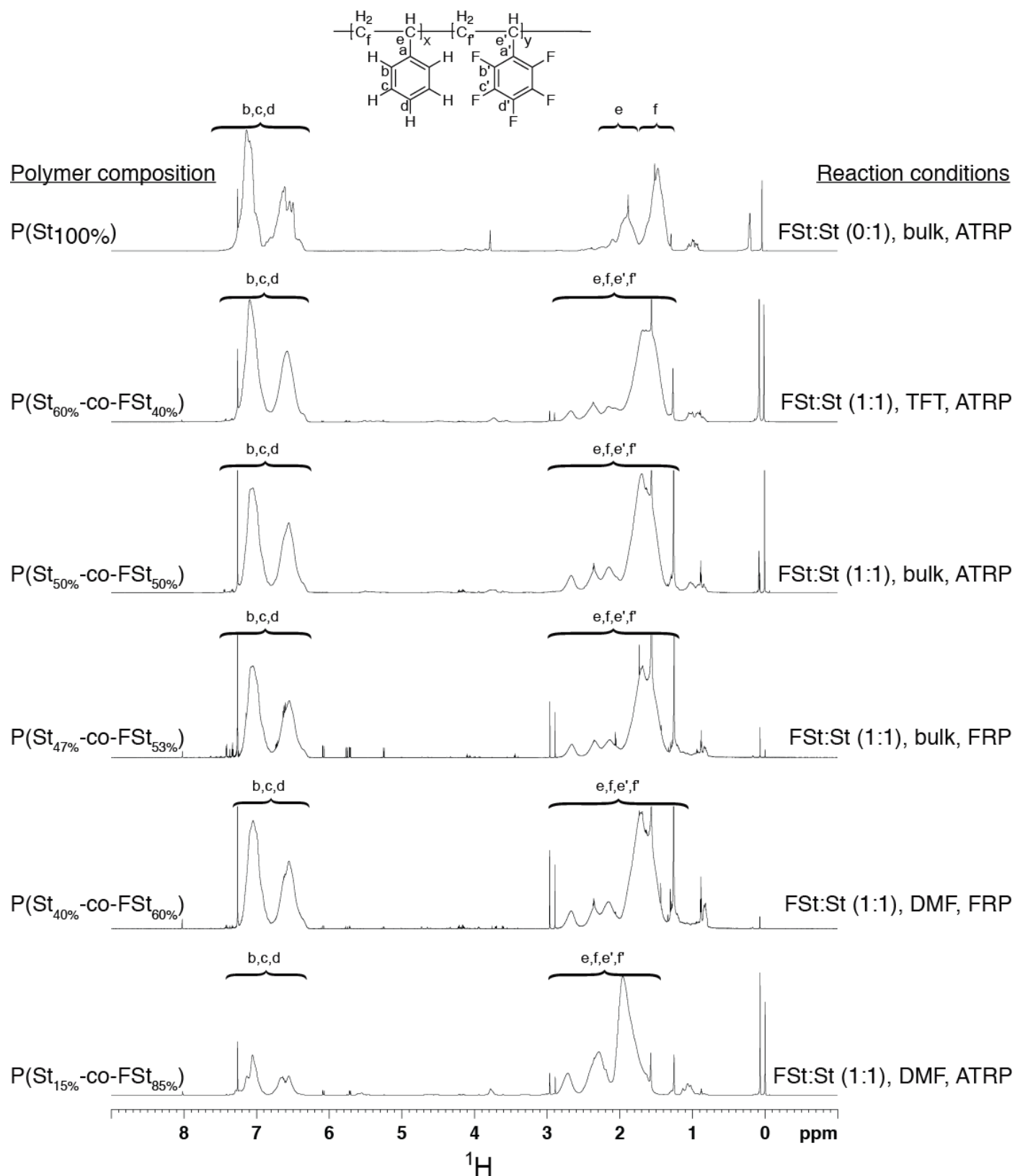
S 12. Aggregate sizing of monomer/solvent mixtures.

## 8. Glass transition temperatures of various St-FSt copolymers

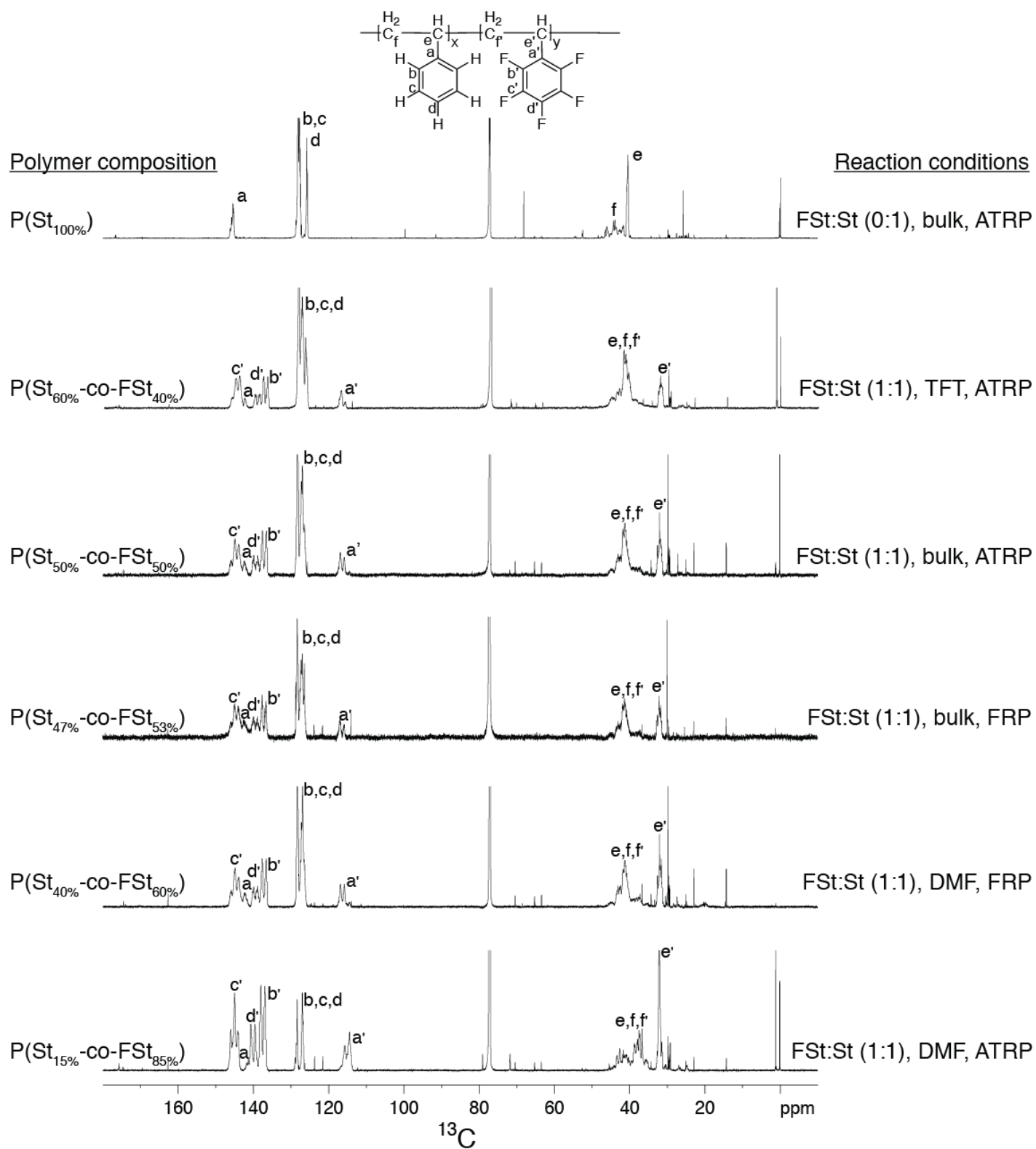


S 13. Glass transition temperatures of homopolymers, random and alternating co-polymers, and block co-polymers of St and FSt. The values after the sample name represent the percentage of the respective monomers on a mole basis in the copolymer, as determined by proton NMR. The far-right cross-hatched bars refer to random copolymers produced by FRP with AIBN. All other samples were prepared by ATRP with BP.

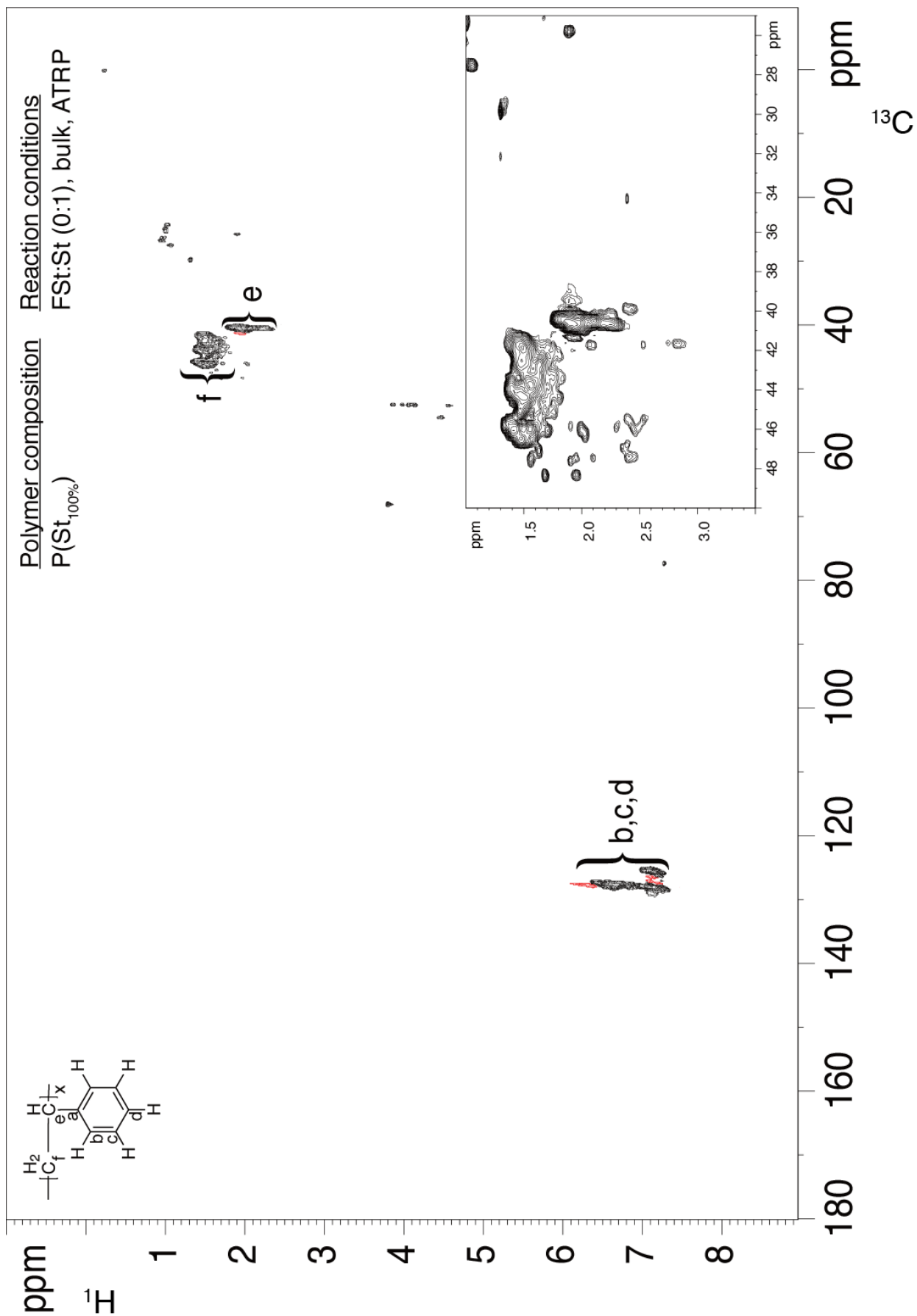
## 9. Determining the alternation mode of copolymers by HMBC NMR



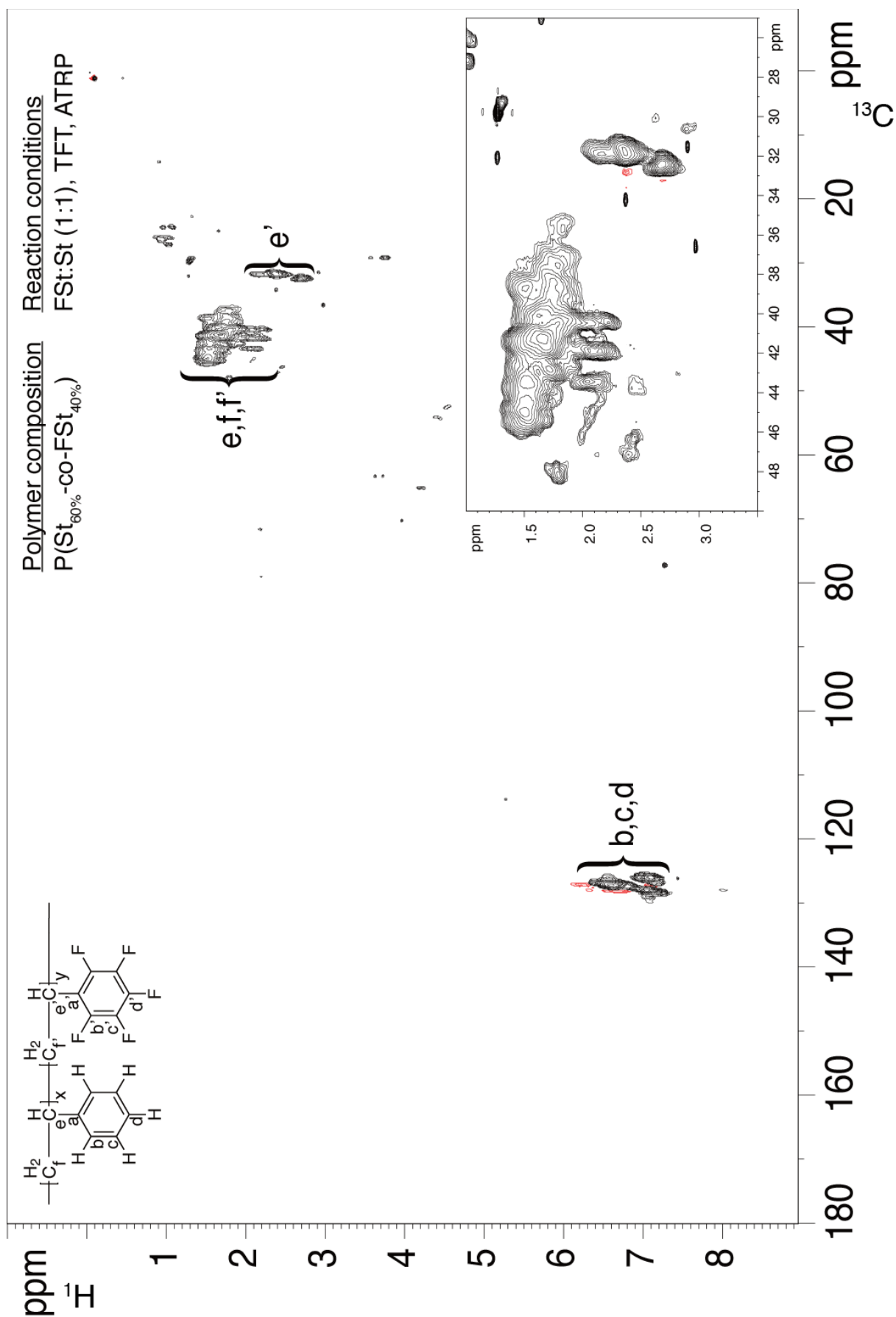
S 14. <sup>1</sup>H spectra (950 MHz) for PSt and various P(FSt-St) copolymers.



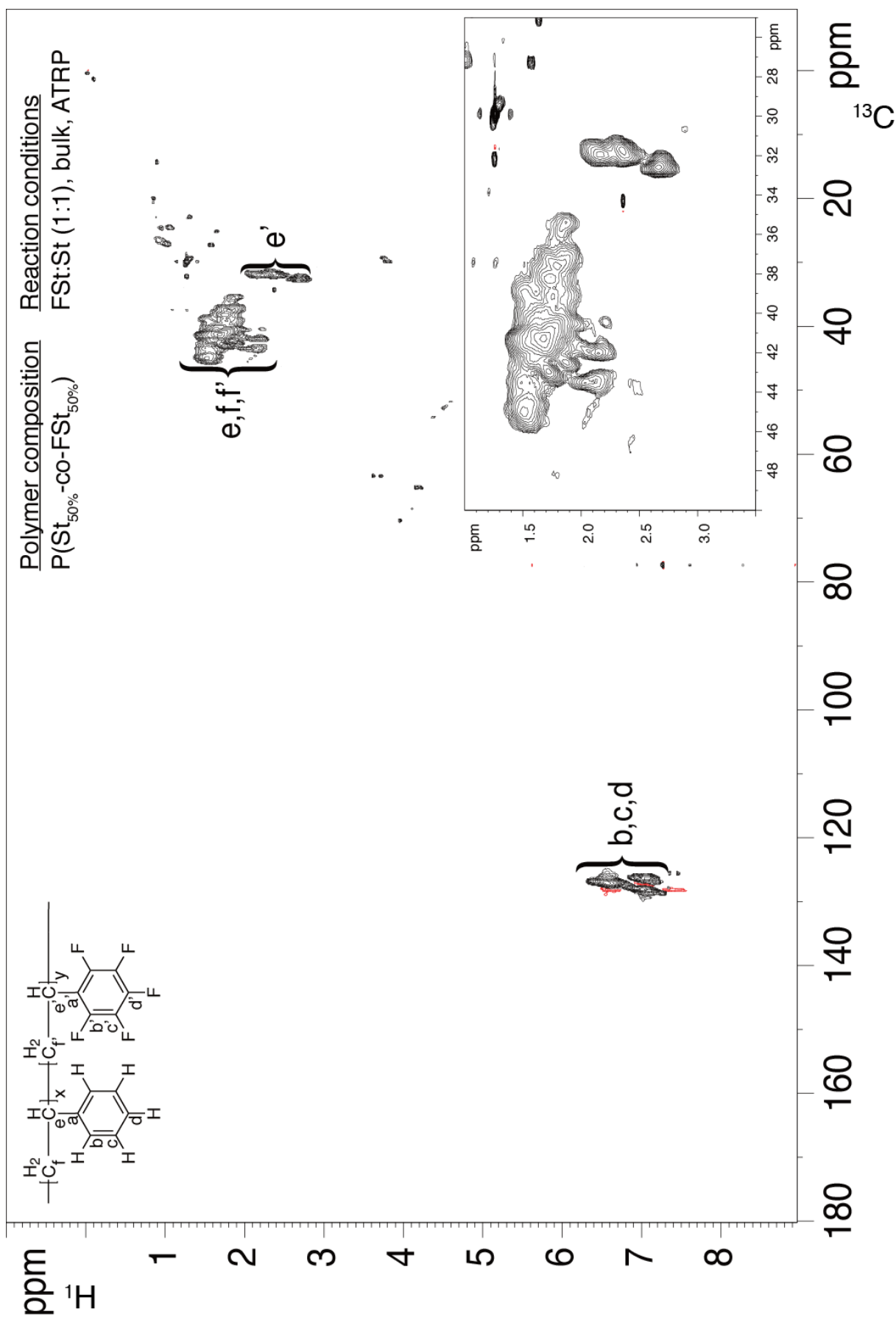
S 15.  $^{13}\text{C}$  spectra (239.4 MHz) for PSt and various P(FSt-St) copolymers.



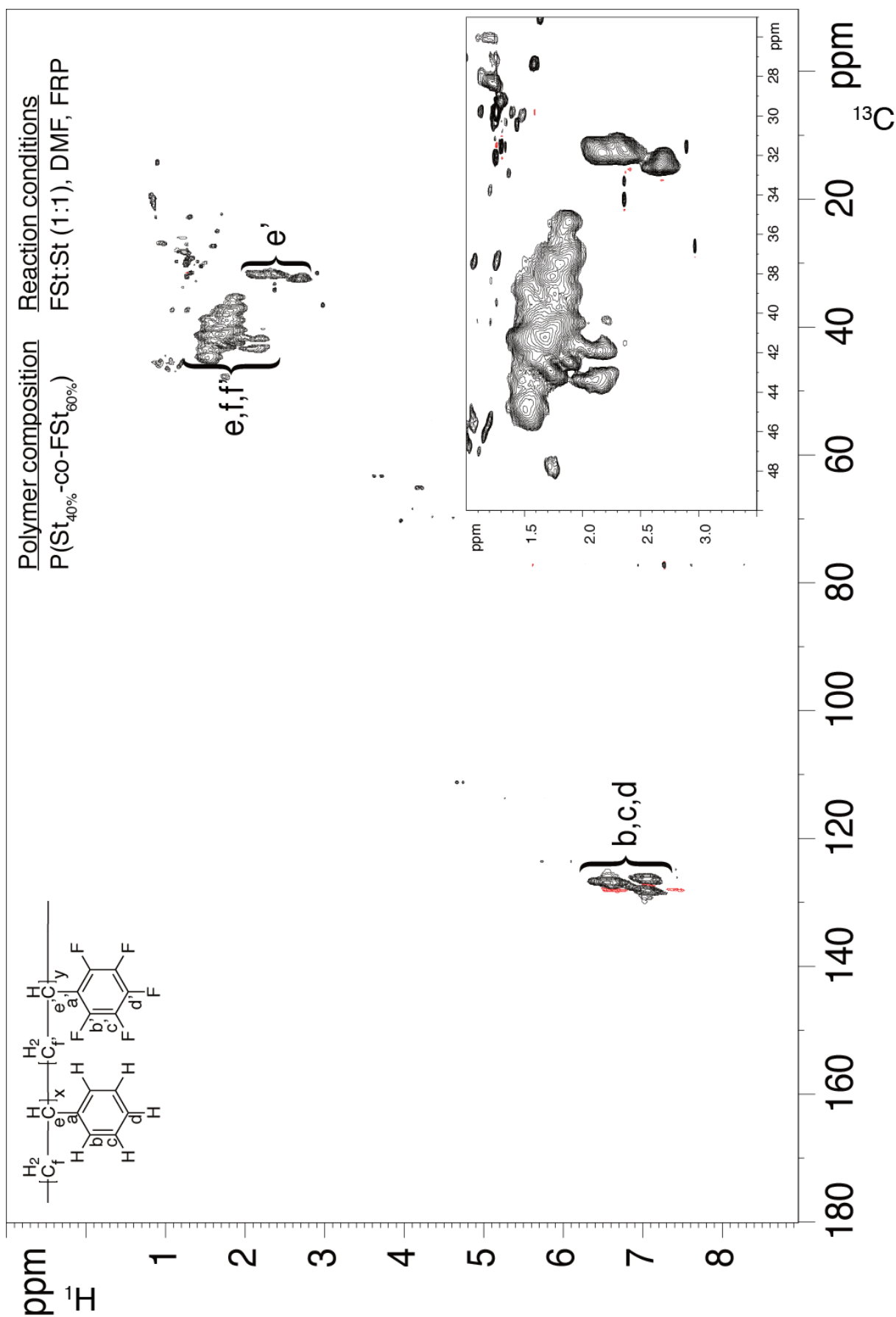
S 16.  $^1\text{H}$ - $^{13}\text{C}$  HSQC spectrum of PSt, prepared by ATRP with BP initiator in bulk.



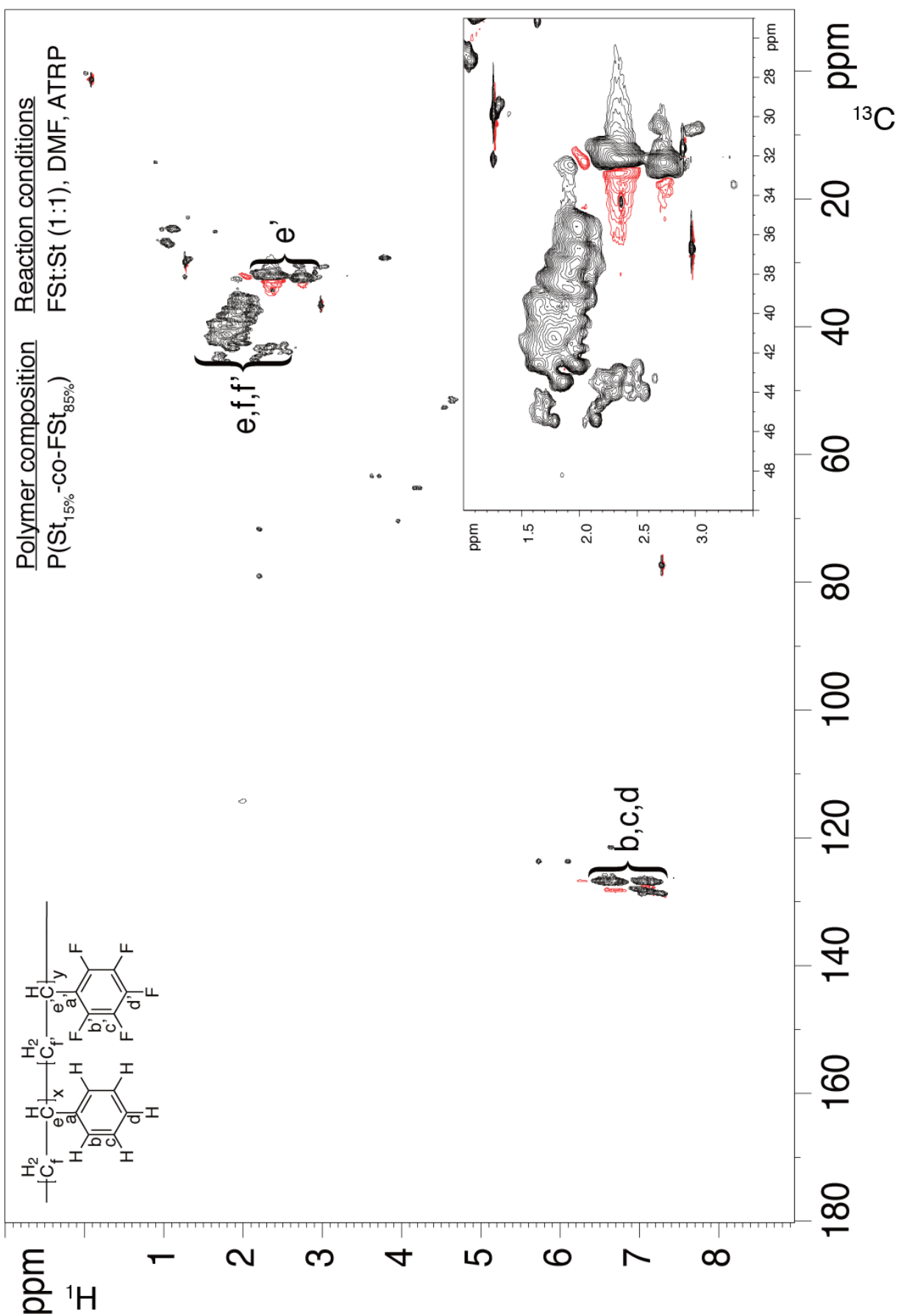
S 17. <sup>1</sup>H-<sup>13</sup>C HSQC spectrum of P(St<sub>60%</sub>-FSt<sub>40%</sub>), prepared by ATRP with BP initiator in TFT.



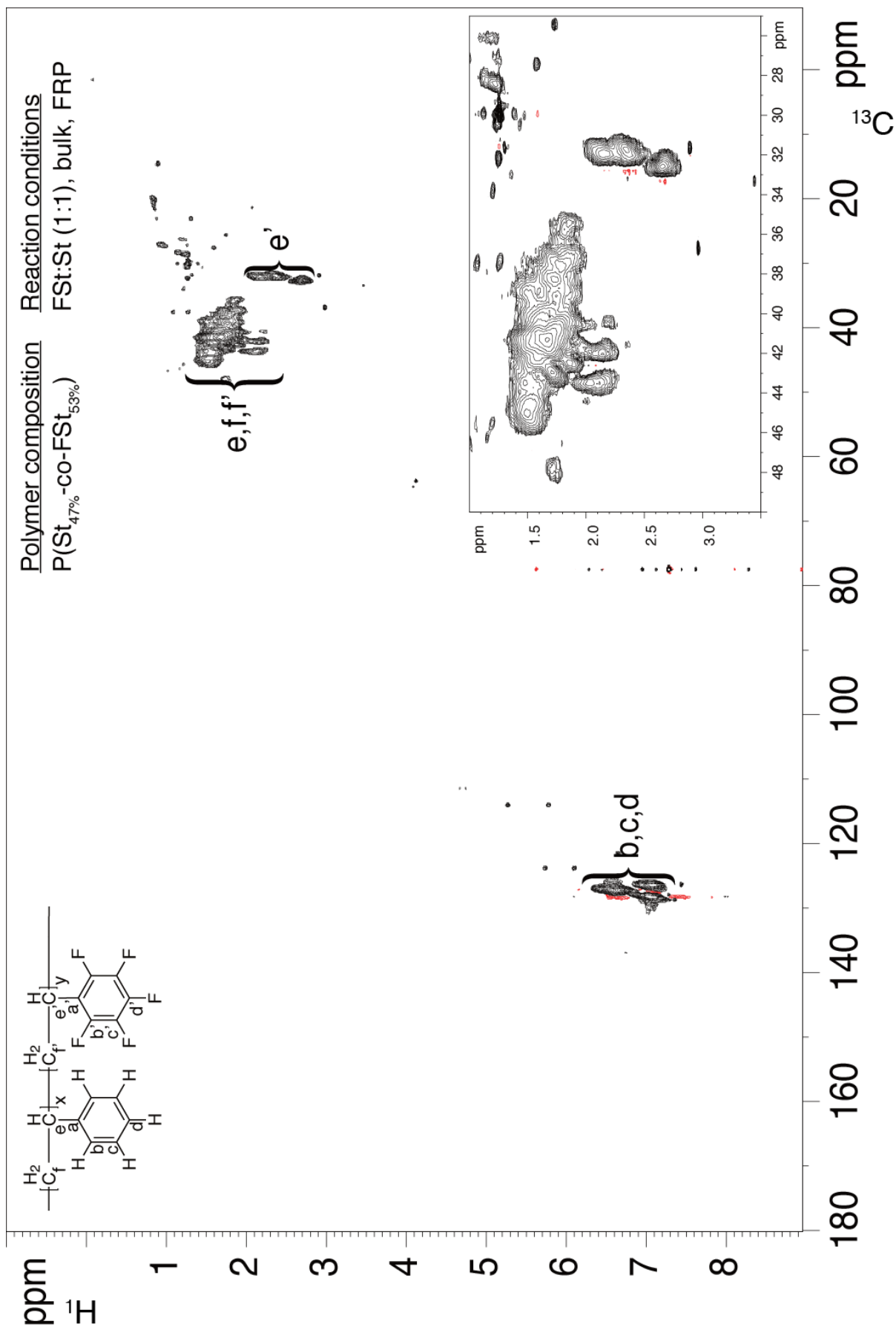
S 18.  $^1\text{H}$ - $^{13}\text{C}$  HSQC spectrum of P( $\text{St}_{50\%}$ -FSt $_{50\%}$ ), prepared by ATRP with BP initiator, in bulk.



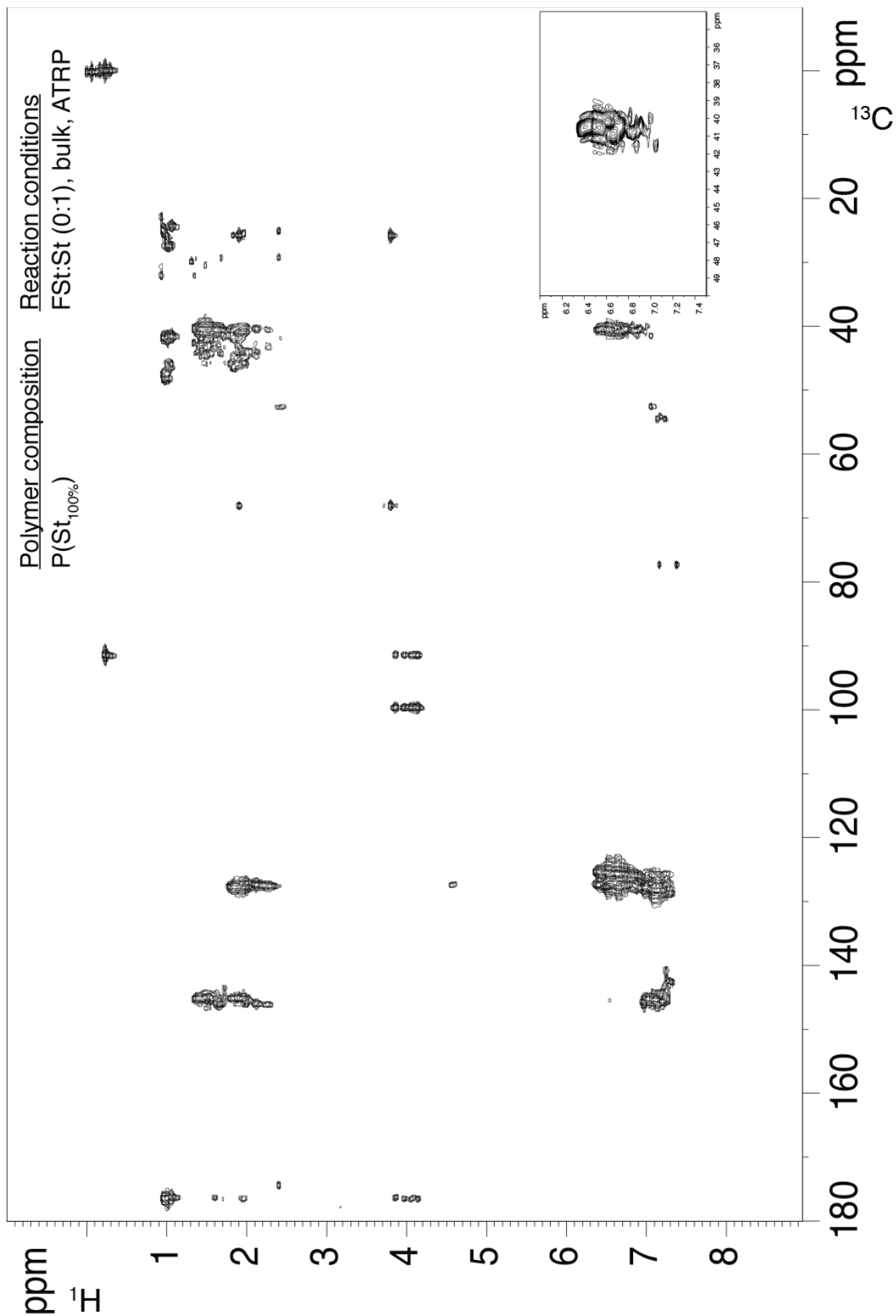
S 19. <sup>1</sup>H-<sup>13</sup>C HSQC spectrum of P(St<sub>40%</sub>-FSt<sub>60%</sub>), prepared by FRP with AIBN initiator in DMF.



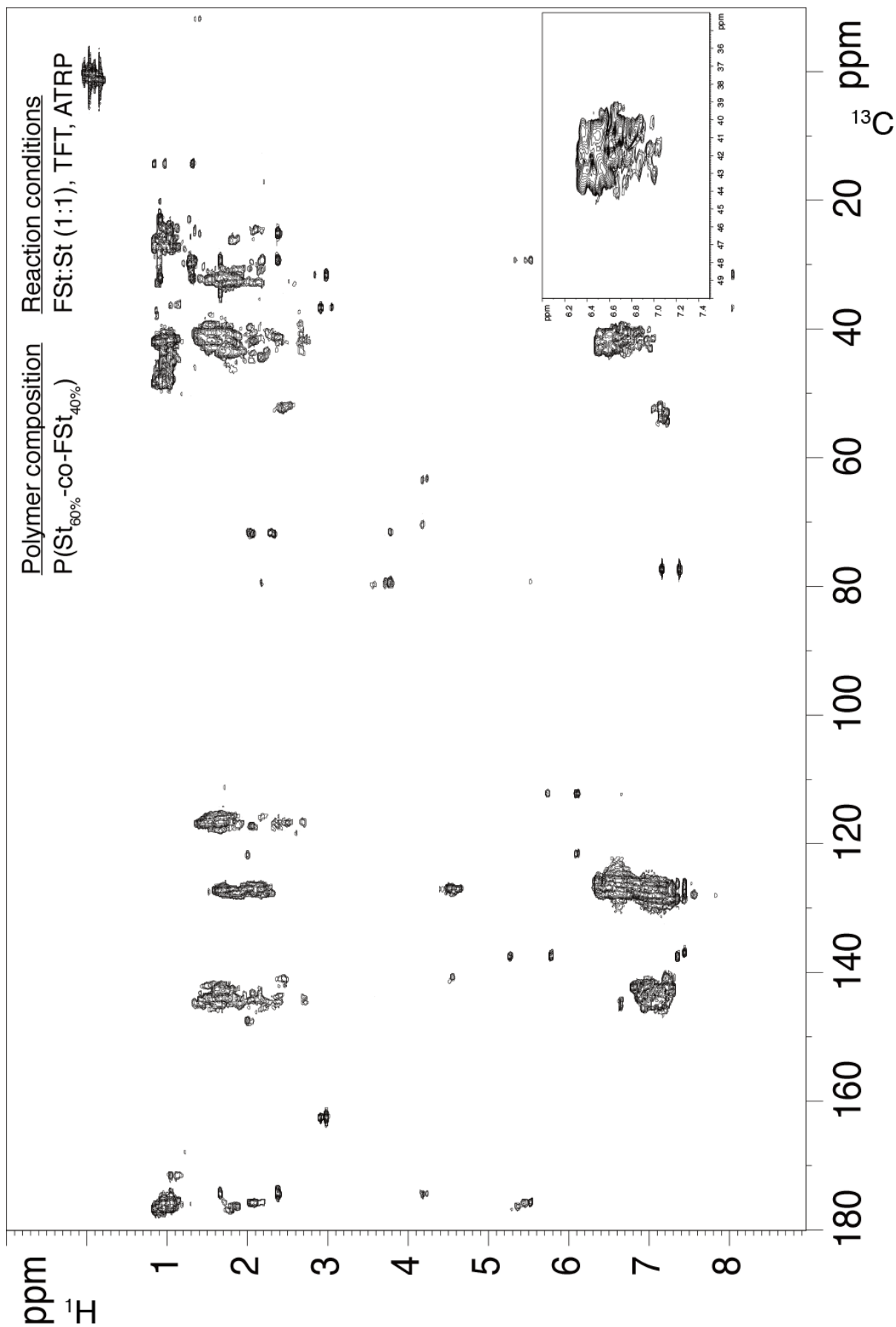
S 20. <sup>1</sup>H-<sup>13</sup>C HSQC spectrum of P(St<sub>15%</sub>-FSt<sub>85%</sub>), prepared by ATRP with BP initiator in DMF (sampled at 15% conversion).



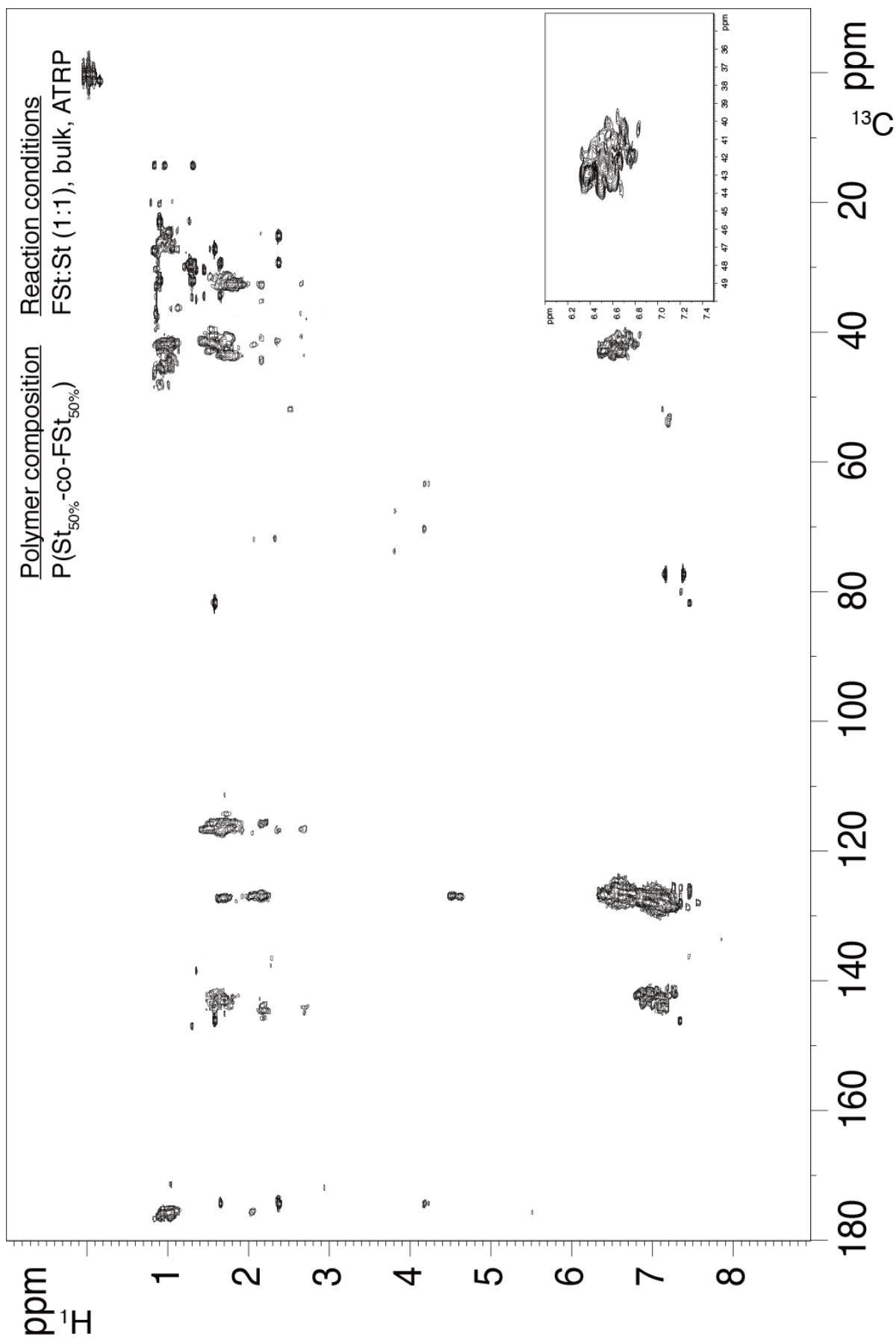
S 21. <sup>1</sup>H-<sup>13</sup>C HSQC spectrum of P(St<sub>47%</sub>-FSt<sub>53%</sub>), prepared by FRP with AIBN initiator, in bulk.



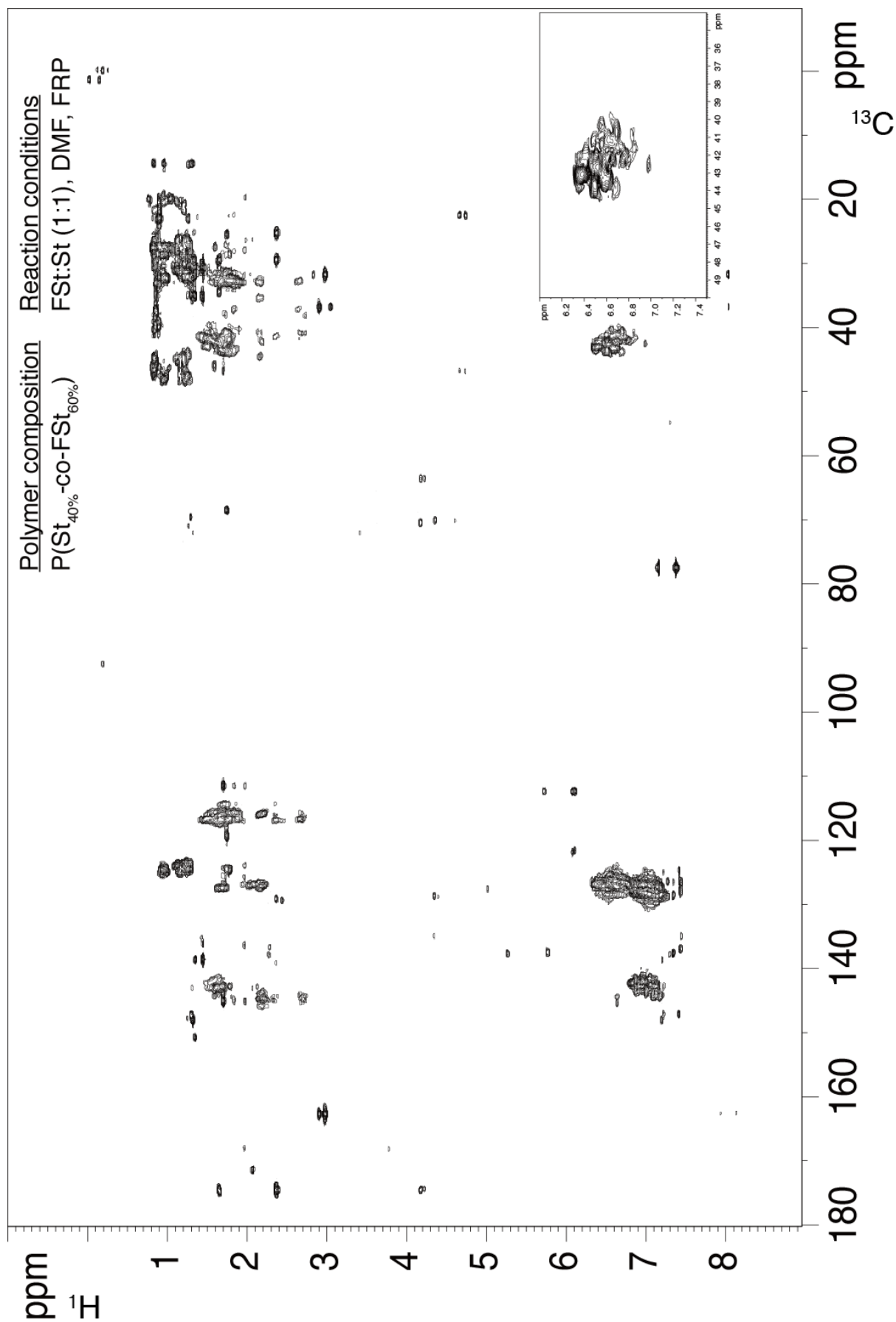
S 22.  $^1\text{H}$ - $^{13}\text{C}$  HMBC spectrum of PSt, prepared by ATRP with BP initiator in bulk.



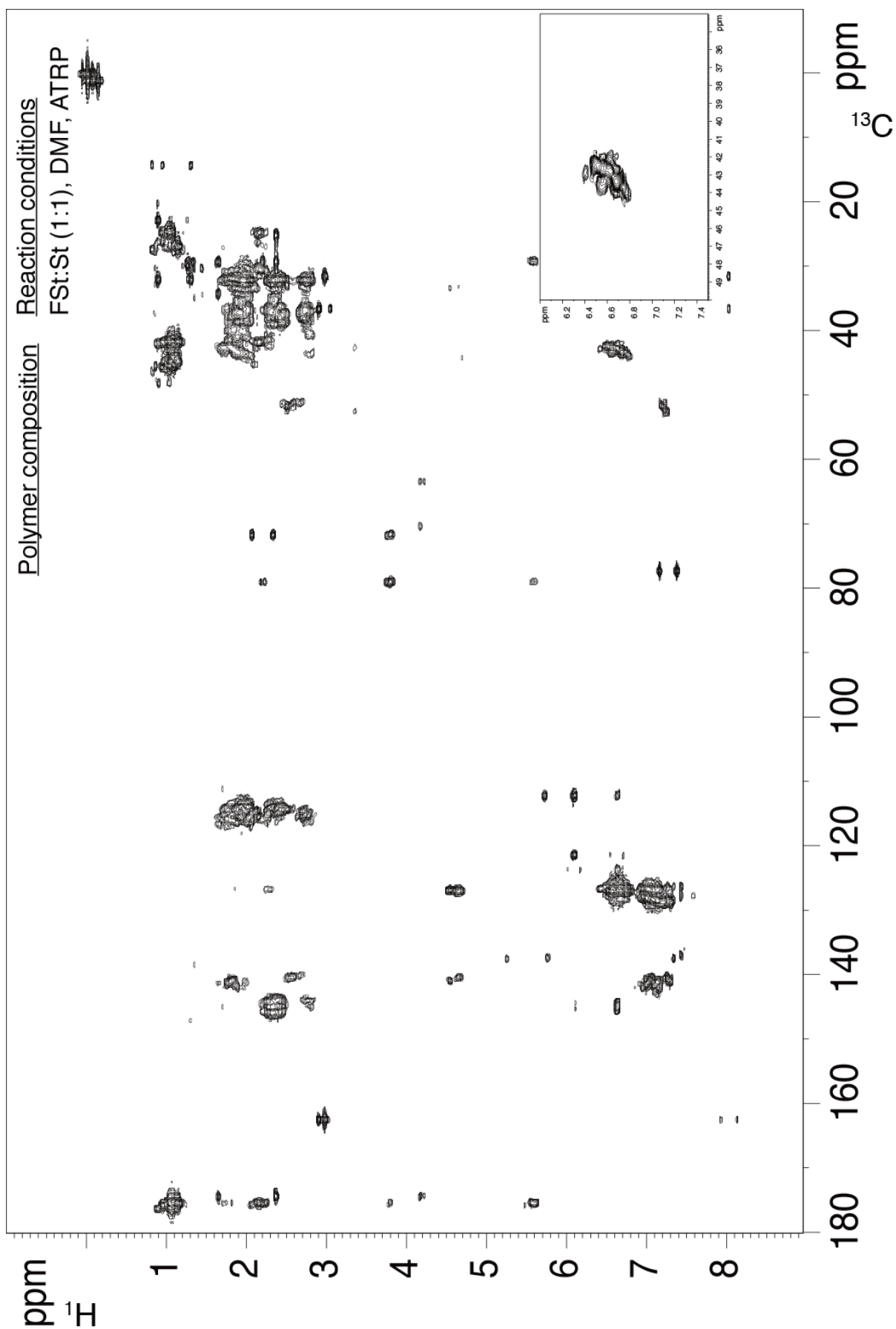
S 23. <sup>1</sup>H-<sup>13</sup>C HMBC spectrum of P(St<sub>60%</sub>-FSt<sub>40%</sub>), prepared by ATRP with BP initiator in TFT.



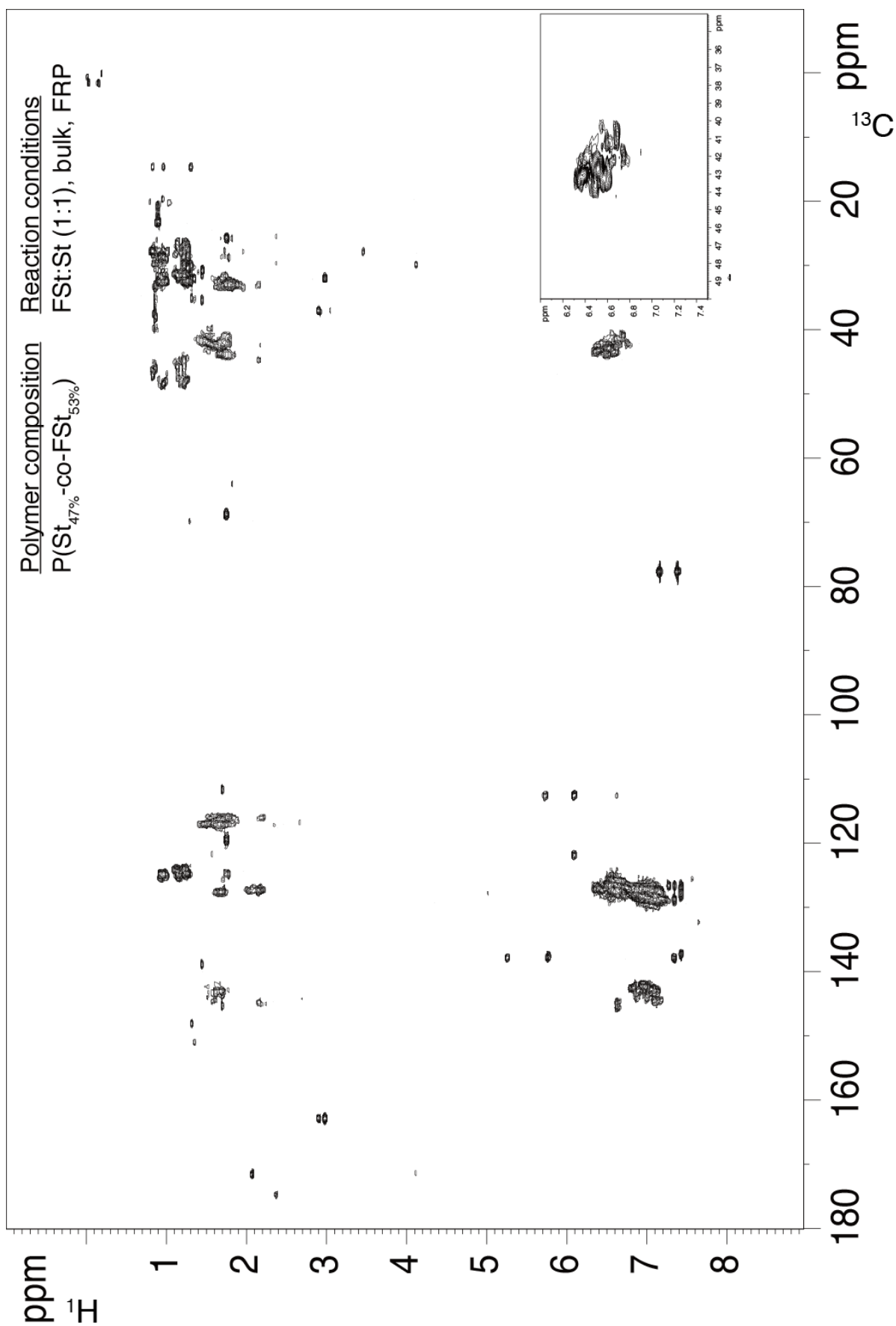
S 24. <sup>1</sup>H-<sup>13</sup>C HMQC spectrum of P(St<sub>50%</sub>-FSt<sub>50%</sub>), prepared by ATRP with BP initiator, in bulk.



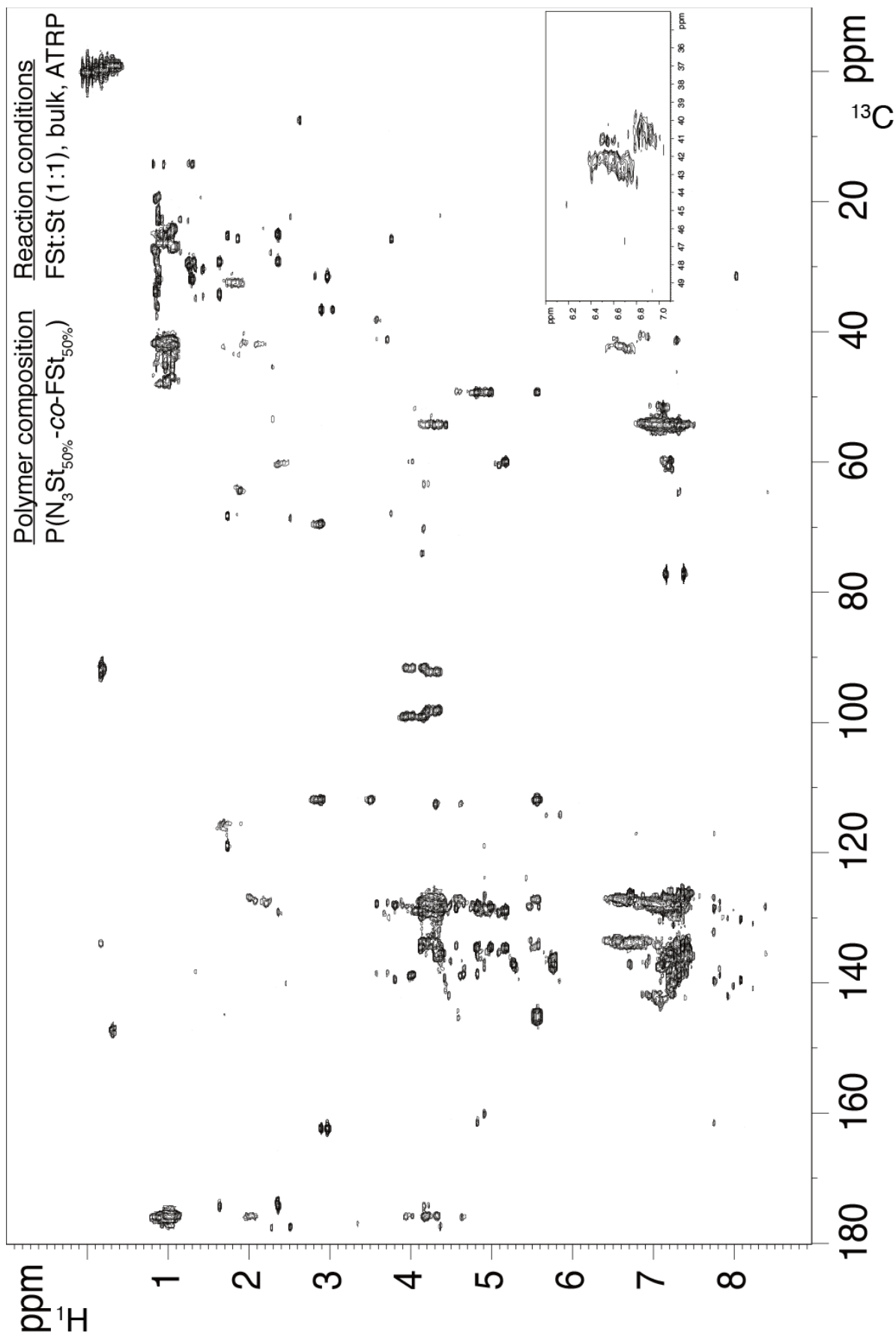
S 25. <sup>1</sup>H-<sup>13</sup>C HMBC spectrum of P(St<sub>40%</sub>-FSt<sub>60%</sub>), prepared by FRP with AIBN initiator in DMF.



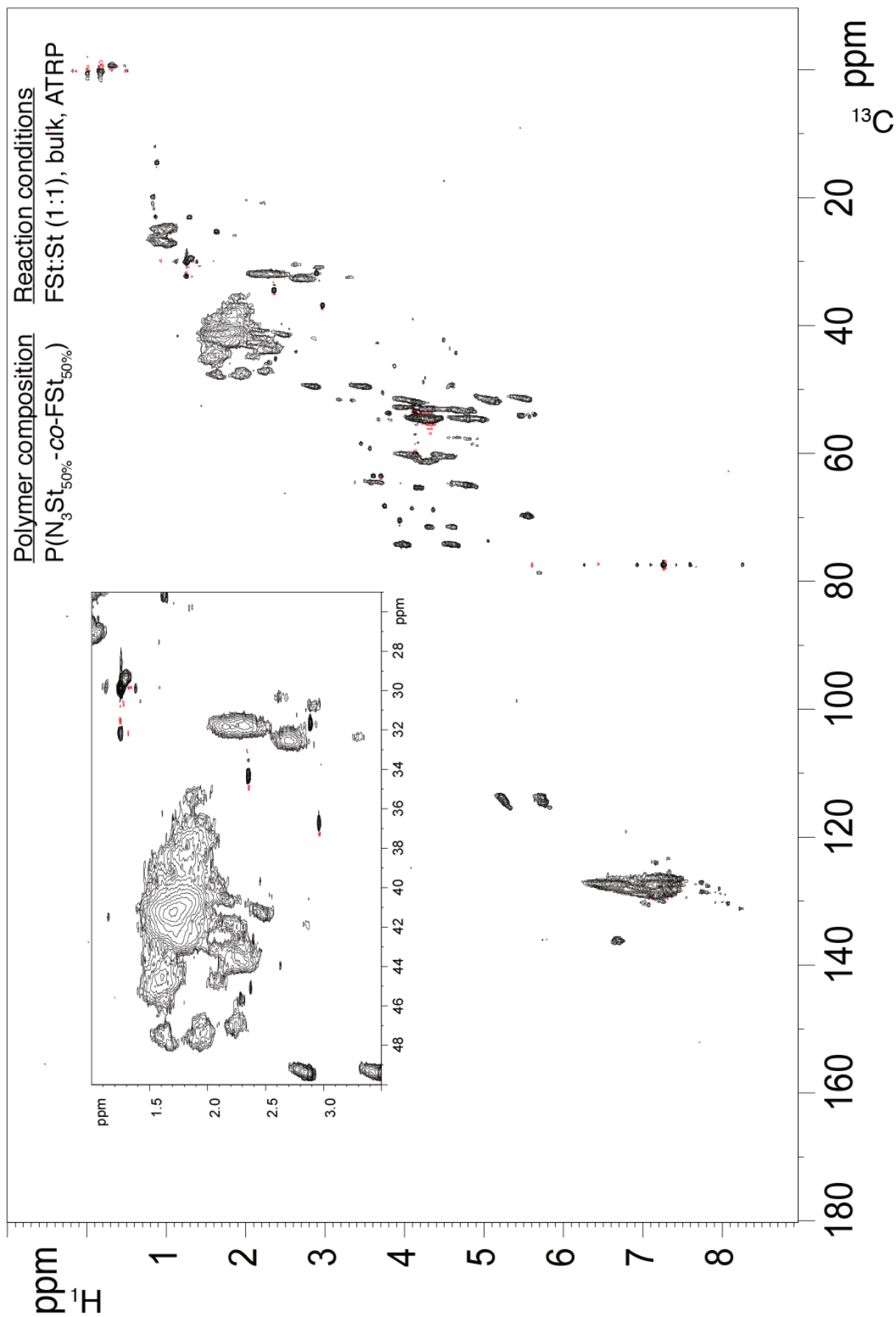
S 26. <sup>1</sup>H-<sup>13</sup>C HMBC spectrum of P(St<sub>15%</sub>-FSt<sub>85%</sub>), prepared by ATRP with BP initiator in DMF (sampled at 15% conversion).



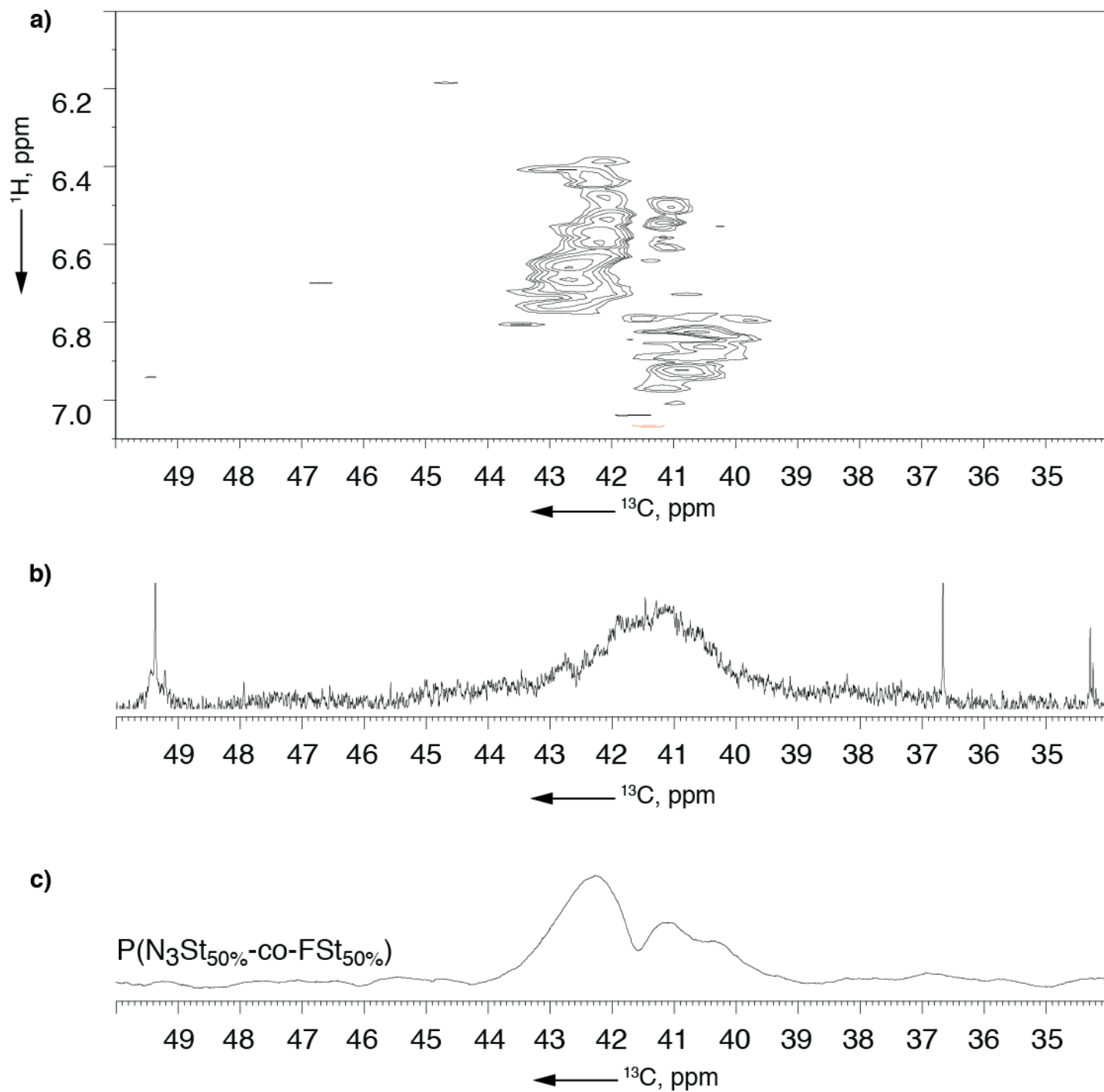
S 27. <sup>1</sup>H-<sup>13</sup>C HMBC spectrum of P(St<sub>47%</sub>-FSt<sub>53%</sub>), prepared by FRP with AIBN initiator, in bulk.



S 28. <sup>1</sup>H-<sup>13</sup>C HMBC spectrum of P(N<sub>3</sub>St<sub>50%</sub>-FSt<sub>50%</sub>), prepared by ATRP with TP initiator in bulk.



S 29. <sup>1</sup>H-<sup>13</sup>C HSQC spectrum of P(N<sub>3</sub>St<sub>50%</sub>-FSt<sub>50%</sub>), prepared by ATRP with TP initiator in bulk.

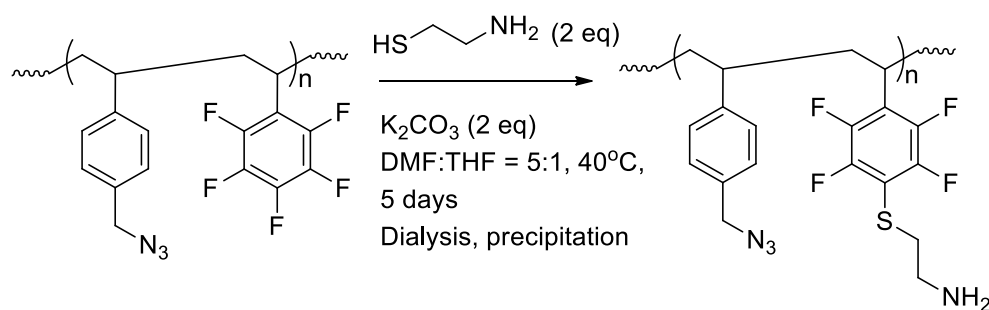


S 30. a) Expanded  $^1\text{H}$ - $^{13}\text{C}$  HMBC spectrum of  $\text{P}(\text{N}_3\text{St}_{50\%}\text{-co-FSt}_{50\%})$ , prepared by ATRP with TP initiator in bulk; b) Expanded  $^{13}\text{C}$  spectrum of the same polymer (35-49 ppm); c)  $^{13}\text{C}$  projection of the same region of the HMBC spectrum. The resonance of the backbone CH can be clearly interpreted. The polymer is mostly alternating, with the shoulder on the right suggesting a degree of randomness.

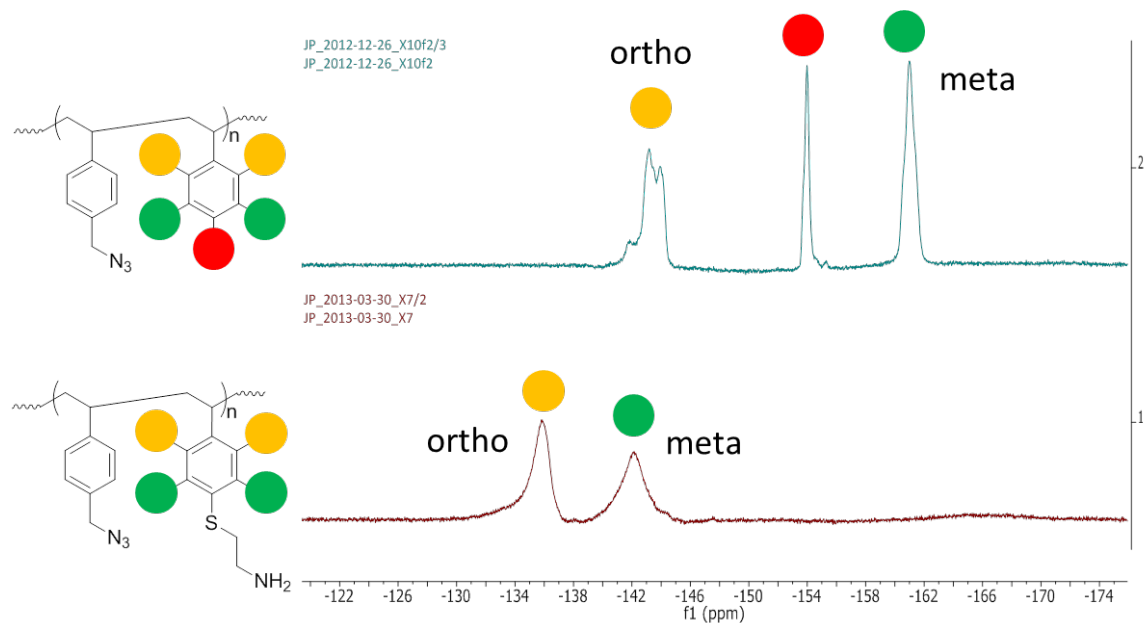
## 10. Functionalization of P(N<sub>3</sub>St-*alt*-FSt) copolymer and catalysis

### General procedure for cysteamine attachment by thiol substitution of *para*-F of FSt

The general procedure is described in S 31. In a dry and clean schlenk tube P(N<sub>3</sub>St-*alt*-FSt) copolymer (1.7 g, M<sub>n</sub> = 5000, PDI = 1.2, 9.6 mmol on an average 1:1 monomer basis, 1 eq.) was dissolved in 5 mL dry THF. After complete dissolution of the polymer in the THF, dry DMF (5 mL) was added. Cysteamine (1.86 g, 24 mmol, 2.5 eq.) is added along with a further 5 mL dry DMF. The tube is purged with argon for 2 minutes. After the cysteamine is completely dissolved, previously dried and ground K<sub>2</sub>CO<sub>3</sub> (2.92 g, 28.9 mmol, 3 eq.) is added under argon flow and the heterogeneous mixture is stirred rapidly under argon for 5 days. After 5 days, the reaction mixture is filtered through 0.45 micron syringe filter to remove the K<sub>2</sub>CO<sub>3</sub>. The reaction mixture is then dialyzed (re-generated cellulose tubing, 1000 g/mol cut-off) against a vast excess of DMF for several days to remove excess cysteamine. The mixture is concentrated at 40°C under vacuum, using the addition of toluene to aid in DMF removal. When ~ 2 mL of the DMF/polymer solution remains, the residue is precipitated into petroleum ether or diethyl ether, and the obtained solid is dried under vacuum at room temperature. The substitution of cysteamine onto the FSt moiety of the polymer was successful as shown by complete disappearance of the *para*-fluorine resonance from <sup>19</sup>F spectra of the functionalized polymer as demonstrated in S 32.



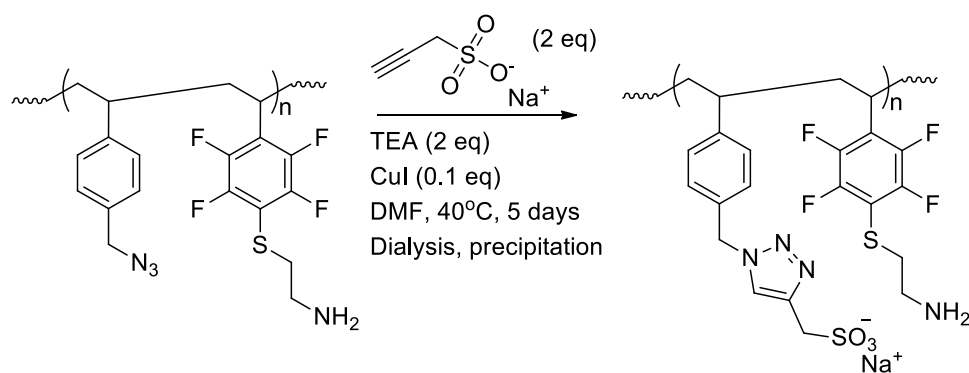
S 31. Reaction scheme for thiol substitution of cysteamine onto a P(N<sub>3</sub>St-*alt*-FSt) polymer.



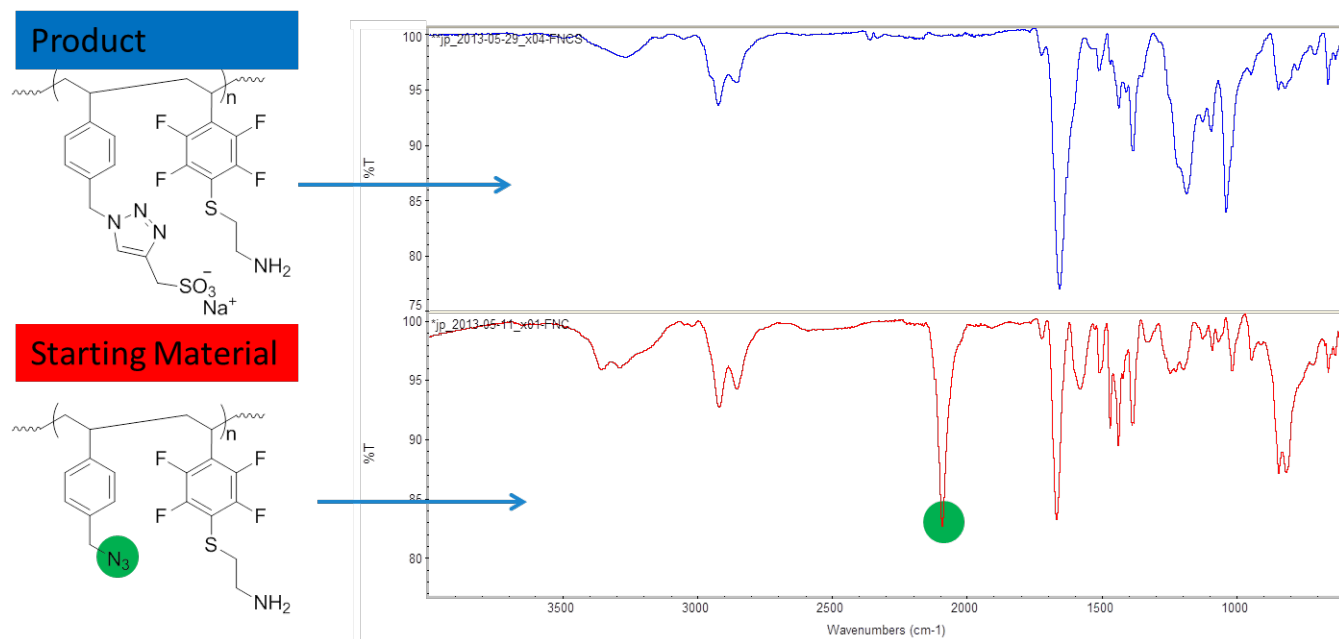
S 32. Comparison of <sup>19</sup>F spectra of starting P(N<sub>3</sub>St-*alt*-FSt) and cysteamine functionalized product after thiol-substitution. Solvent was DMF-*d*<sub>6</sub>.

### General procedure for sulfonate attachment by CuAAC onto $N_3$ St moiety of the polymer

The general procedure is described in S 33. The P( $N_3$ St-alt-FSt) copolymer (0.5 g, 4.8 mmol on an average 1:1  $N_3$ St and FSt-cysteamine monomer basis, 1 eq.) which had been functionalized with cysteamine as described in the previous step was dissolved in dry DMF (10 mL) in a clean and dry schlenk tube. Sodium propargyl sulfonate (1.023 g, 7.2 mmol, 1.5 eq.) and TEA (0.97 g, 1.34 mL, 9.6 mmol, 2 eq.) were added and the mixture dissolved. The mixture was subject to 3 x freeze, pump, thaw cycles. On a 4<sup>th</sup> freeze, CuI (91.4 mg, 0.48 mmol, 0.1 eq.) was added under nitrogen. After an additional pumping period, the flask was backfilled with nitrogen, thawed and placed in a 40°C oil bath and stirred. After 3 days, FTIR analysis of samples (precipitated into DEE) indicated completion of the reaction by disappearance of the azide peak at 2100  $\text{cm}^{-1}$  as shown in S 34. After removal of the flask from the oil bath, the reaction mixture was passed through a short column of basic alumina and subsequently dialyzed (regenerated cellulose tubing, 1000 g/mol cut-off) against a vast excess of DMF for several days to remove excess sodium propargyl sulfonate. Addition of toluene resulted in precipitation of the polymer, which was recovered by centrifugation, washed with DEE and dried under vacuum at room temperature.



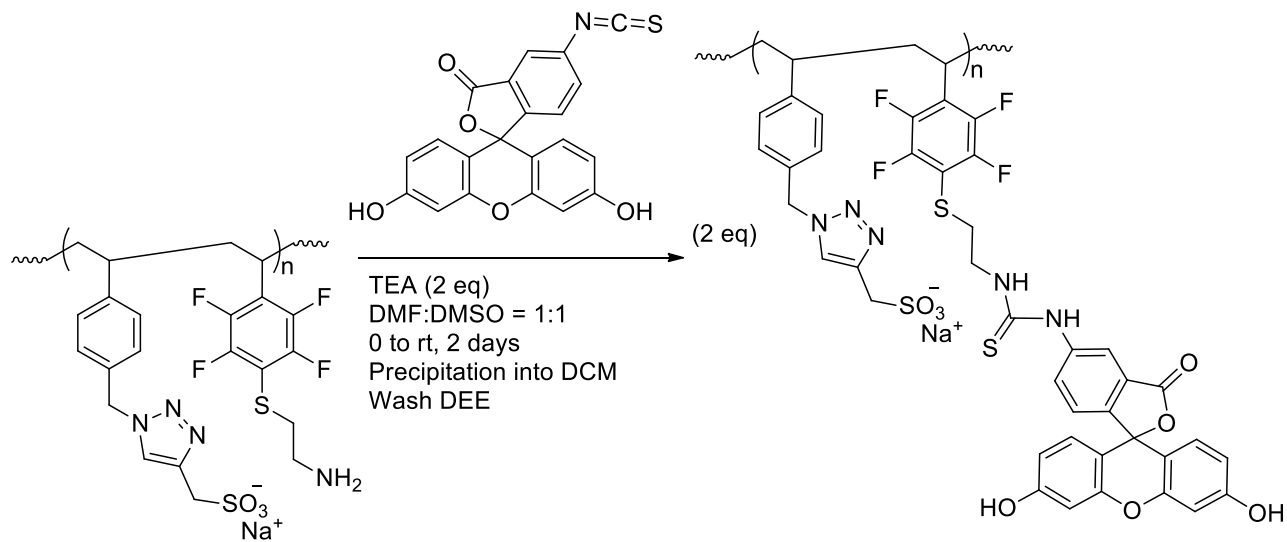
S 33. Reaction scheme for CuAAC mediated attachment of a sulfonate residue to a P( $N_3$ St-alt-FSt) previously functionalized with a cysteamine residue.



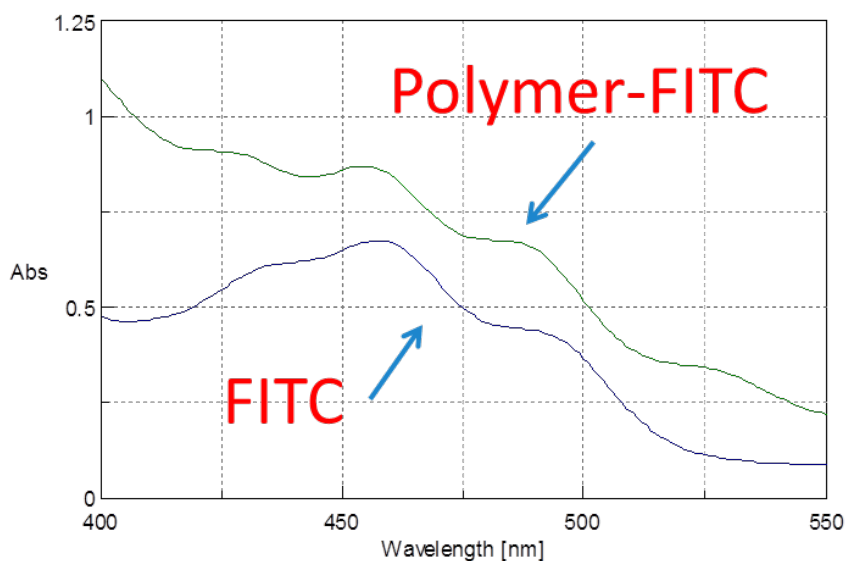
S 34. Comparison of ATR-FTIR spectra of the starting material and product polymers from the CuAAC mediated attachment of a sulfonate residue to a P( $N_3$ St-alt-FSt) polymer which contains a cysteamine residue.

### Check of primary-amine stability of the cysteamine residue by reaction with FITC

We were concerned that the primary amine on the cysteamine residue may not have survived the CuAAC conditions (possible cross-linking). Therefore facile visualization using FITC functionalization was undertaken (S35). Briefly, cysteamine and sulfonate functionalized copolymer (50 mg, 0.2 mmol, 1 eq.) was dissolved (1:1, DMF:DMSO, 5 mL) containing TEA (27 mg, 37 microliter, 0.27 mmol, 1.3 eq.). After cooling the mixture to 0°C a solution of FITC (104 mg in 2 mL dry DMF, 0.27 mmol, 2 eq.) was added dropwise under nitrogen flow with vigorous stirring, allowing the mixture to come to room temperature over a reaction period of 2 days. After this time, the reaction mixture was precipitated by the addition of DCM. The polymer was recovered by centrifugation, washed with DEE and dried under vacuum at room temperature. UV-Vis of the resultant polymer in DMSO revealed the successful attachment of FITC which indicates stability of the primary amine residues (S 36).



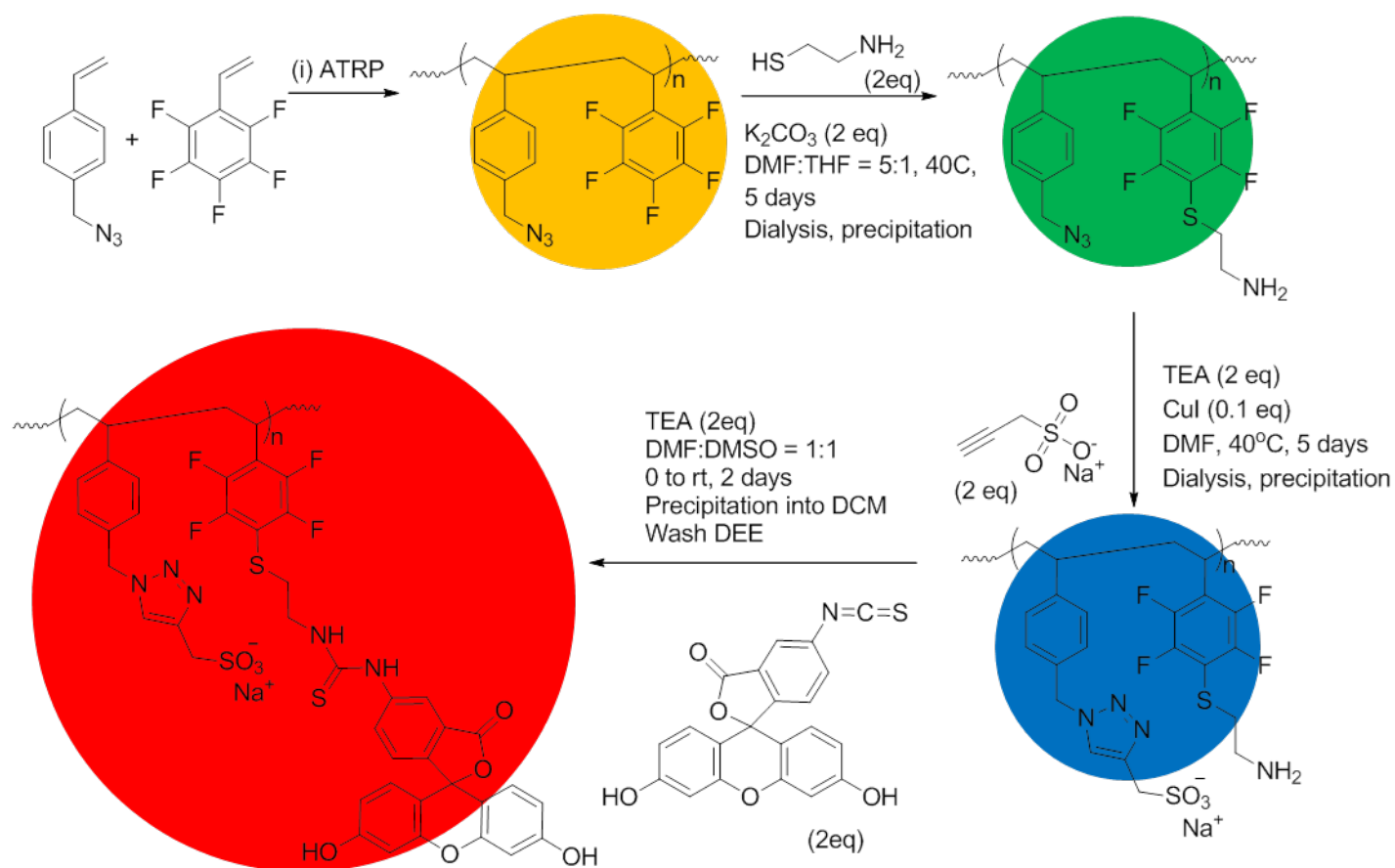
S35. Reaction scheme for FITC functionalization of P(N<sub>3</sub>St-*alt*-FSt) which has been previously functionalized with cysteamine and sulfonate residues.



S 36. Truncated UV-Vis spectra of molecular FITC and FITC functionalized copolymer of P(N<sub>3</sub>St-*alt*-FSt) which has been previously functionalized with cysteamine and sulfonate residues. Green-line (Polymer-FITC, 13.5 mg/mL DMSO); blue-line (FITC, 2.75 mg/mL DMSO).

### Observation of changes in physical appearance of the polymer during functionalization

The overall scheme of functionalization is described in S 37. Definitive changes in the physical appearance of the polymer occurred during the different functionalization steps (S38).



S 37. Scheme of selective attachment of catalysts onto a P(N<sub>3</sub>St-alt-FSt) copolymer by sequential thiol-substitution and CuAAC.



S38. Photos of the change in physical appearance of the polymer during the course of catalyst functionalization color coded to the overall scheme of synthesis.

*General procedure for the Henry reactions.*

Catalyst (4.6 mg, 0.019 mmol, 0.2 eq. of amine and sulfonate groups respectively) was dissolved in DMF (0.5 mL), in a 3 mL reaction vial equipped with a stirring bar. Nitromethane (115 mg, 102  $\mu$ l, 1.9 mmol, 20 eq.) and hexadecane (10  $\mu$ l), benzaldehyde (10 mg, 10  $\mu$ l, 0.094 mmol, 1 eq.) were added sequentially with rapid stirring. An initial sample for GC-MS was taken, after which the sample was placed on a 90 °C hotplate. After 12 hours, a final sample for GC-MS characterization was taken.

## 11. References

- (1) Ouadahi, K.; Allard, E.; Oberleitner, B.; Larpent, C. *J Polym Sci Pol Chem* **2012**, *50*, 314.
- (2) Velcicky, J.; Lanver, A.; Lex, J.; Prokop, A.; Wieder, T.; Schmalz, H.-G. *Chemistry – A European Journal* **2004**, *10*, 5087.
- (3) Sorg, A.; Siegel, K.; Brückner, R. *Chemistry – A European Journal* **2005**, *11*, 1610.
- (4) Bernard, S.; Defoy, D.; Dory, Y. L.; Klarskov, K. *Bioorganic & Medicinal Chemistry Letters* **2009**, *19*, 6127.
- (5) Eugene, D. M.; Grayson, S. M. *Macromolecules* **2008**, *41*, 5082.
- (6) Fielding, L. *Tetrahedron* **2000**, *56*, 6151.
- (7) Hanna, M. W.; Ashbaugh, A. L. *The Journal of Physical Chemistry* **1964**, *68*, 811.
- (8) Rose, N. J.; Drago, R. S. *Journal of the American Chemical Society* **1959**, *81*, 6138.
- (9) Wachter, H. N.; Fried, V. *J. Chem. Educ.* **1974**, *51*, 798.
- (10) Nishimura, S.; Nagai, A.; Takahashi, A.; Narita, T.; Hagiwara, T.; Hamana, H. *Polymer Journal* **1990**, *22*, 171.
- (11) Pryor, W. A.; Huang, T.-L. *Macromolecules* **1969**, *2*, 70.
- (12) Pugh, C.; Paz-Pazos, M.; Tang, C. N. *Journal of Polymer Science Part A: Polymer Chemistry* **2009**, *47*, 331.
- (13) Pugh, C.; Tang, C. N.; Paz-Pazos, M.; Samtani, O.; Dao, A. H. *Macromolecules* **2007**, *40*, 8178.
- (14) ten Brummelhuis, N.; Weck, M. *Acs Macro Letters* **2012**, *1*, 1216.
- (15) Mayo, F. R.; Lewis, F. M. *Journal of the American Chemical Society* **1944**, *66*, 1594.
- (16) Odian, G. In *Principles of Polymerization*; John Wiley & Sons, Inc.: 2004, p 464.
- (17) Fineman, M.; Ross, S. D. *Journal of Polymer Science* **1950**, *5*, 259.
- (18) Litwinienko, G.; Beckwith, A. L. J.; Ingold, K. U. *Chemical Society Reviews* **2011**, *40*, 2157.
- (19) Olaj, O. F.; Schnöll-Bitai, I. *Monatshefte fuer Chemie* **1999**, *130*, 731.
- (20) Karad, P.; Schneider, C. *J Polym Sci Pol Chem* **1978**, *16*, 1137.
- (21) Seiner, J. A.; Litt, M. *Macromolecules* **1971**, *4*, 308.
- (22) Baur, M. E.; Horsma, D. A.; Knobler, C. M.; Perez, P. *The Journal of Physical Chemistry* **1969**, *73*, 641.
- (23) In *Landolt-Börnstein: Numerical Data and Functional Relationships in Science and Technology*; Wolhlfarth, C., Lechner, M. D., Eds.; Springer: Berlin, 2008.
- (24) Viswanath, D. S.; Ghosh, T. K.; Prasad, D. L.; Ndutt, N. V. K.; Rani, K. Y. *Viscosity of Liquids: Theory, Estimation, Experiment, and Data*; Springer: Dordrecht, The Netherlands, 2007.
- (25) In *Handbook of Electrochemistry*; Zosk, C. G., Ed.; Elsevier: 2007.